Compressional and Shear Wave Velocity Versus Depth in the San Francisco Bay Area, California: Rules for USGS Bay Area Velocity Model 05.0.0

By Thomas M. Brocher[1]

Open-File Report 05–1317

2005

U.S. DEPARTMENT OF THE INTERIOR
U.S. GEOLOGICAL SURVEY

[1]Menlo Park, Calif.

ABSTRACT

This report summarizes and documents empirical compressional wave velocity (Vp) versus depth relationships for several important rock types in northern California used in constructing the new USGS Bay Area Velocity Model 05.0.0 [http://www.sf06simulation.org/]. These rock types include the Jurassic and Cretaceous Franciscan Complex (metagraywacke and greenstones), serpentinites, Cretaceous Salinian and Sierra granites and granodiorites, Jurassic and Cretaceous Great Valley Sequence, and older Cenozoic sedimentary rocks (including the La Honda basin). Similar relations for less volumetrically important rocks are also developed for andesites, basalts, gabbros, and Sonoma Volcanics. For each rock type I summarize and plot the data used to develop the velocity versus depth relationships. These plots document the existing constraints on the proposed relationships.

This report also presents a new empirical Vp versus depth relation derived from hundreds of measurements in USGS 30-m vertical seismic profiles (VSPs) for Holocene and Plio-Quaternary deposits in the San Francisco Bay area. For the upper 40 m (0.04 km) these mainly Holocene deposits, can be approximated by Vp (km/s) $= 0.7 + 42.968z - 575.8z^2 + 2931.6z^3 - 3977.6z^4$, where z is depth in km. In addition, this report provides tables summarizing these VSP observations for the various types of Holocene and Plio-Quaternary deposits.

In USGS Bay Area Velocity Model 05.0.0 these compressional wave velocity (Vp) versus depth relationships are converted to shear wave velocity (Vs) versus depth relationships using recently proposed empirical Vs versus Vp relations. Density is calculated from Vp using Gardner's rule and relations for crystalline rocks proposed by Christensen and Mooney (1995). Vs is then used to calculate intrinsic attenuation coefficients for shear and compressional waves, Qs and Qp, respectively.

CONTENTS

TABLES

FIGURES

Introduction

The purpose of this report is to present compressional wave velocity versus depth relationships for several important rock types in northern California. These relations were used to populate a new 3D velocity model for northern California (USGS Bay Area Velocity Model 05.0.0 [http://www.sf06simulation.org/]). The model was first constructed as a structural and geologic model that was converted into a compressional and shear wave velocity, density, and intrinsic attenuation model. The 3D velocity model will be used to calculate synthetic strong ground motions for scenario earthquakes in the San Francisco Bay Area, including the 1989 Loma Prieta and the 1906 San Francisco earthquakes.

The rock types examined here include the Jurassic and Cretaceous Franciscan Complex (metagraywacke and greenstone), serpentinites, Cretaceous Salinian and Sierra granites and granodiorites, Jurassic and Cretaceous Great Valley Sequence, older Cenozoic sedimentary rocks (including the La Honda basin). Fortunately, there is a large number of data for granites and Franciscan Complex rocks, which comprise the bulk of the crystalline crust in the San Francisco Bay area. Similar relations for less volumetrically important rocks are also developed for andesites, basalts (both unaltered and metamorphic), gabbros, and Sonoma Volcanics. I also summarize hundreds of compressional and shear wave velocity and density measurements from USGS 30-m vertical seismic profiles (VSP) for Holocene and Plio-Quaternary deposits in the Bay area. Each rock type is described separately and is discussed in alphabetical order. In all the proposed relationships, z represents the subsurface depth in km.

For each rock type I summarize and plot the data used to develop the velocity versus depth relationships. These plots are intended to give the reader a better idea of existing constraints on the proposed relationship. Data compiled to develop these relationships includes VSPs, sonic logs in boreholes, seismic refraction and seismic tomography studies, laboratory measurements of compressional wave velocity (Vp) versus confining pressure, and gravity (density) models. References to the sources of data used in these figures are provided in Table 1,

which identifies the depth of the measurement and type of measurement. Laboratory measurements of Vp versus depth corrected for temperature (Christensen and Mooney, 1995) are an important data source for many rock types. For those measurements I have used values for their average crustal thermal gradient. I also show similar unpublished measurements for samples collected near Loma Prieta that are uncorrected for thermal gradients (N. I. Christensen, writ. comm., 1997).

For each rock type I fit a regression line or curve to the available data, plotted as a function of Vp versus depth. The order of polynomial chosen for each rock type resulted in the highest R^2 obtained for that rock type. In some cases, sparse data were simply fit by eye with linear gradients.

In constructing the new 3D Bay Area Velocity Model, the model is defined in terms of compressional wave velocity (Vp) for which there are many more data than shear wave velocity (Vs). However, for strong ground motions, Vs is usually much more important than Vp because shear and surface waves cause most of the damage (Joyner, 2000). Therefore, these Vp versus depth relationships are converted to Vs versus depth relationships using empirical Vp versus Vs relations recently proposed by Brocher (2005a). In this report, I first summarize these Vp and Vs relations, and then present Vp versus depth curves for the rock types named above.

Although most measurements compiled here are for rocks from Northern California, measurements on volcanics in the Bay area are sparse. Many measurements for basalts compiled here are from Oregon and Washington (Brocher and Horta, 1998; Brocher and Ruebel, 1998; Brocher and Christensen, 2001). Due to the lack of Vp measurements for the Sonoma Volcanics, all of the measurements summarized here for that rock type are from Miocene tuffs near Yucca Mountain, Nevada, for which there are many data.

Finally, a note about the format of this report. Equations previously reported are indicated throughout the text by []. New equations presented here are indicated by ().

Table 1. Vp versus depth data sources

Andesites

Data Source	Depth (km)	Reference	Data Type
Rhyolite, agglomerate	0.00	Fumal (1978)	VSP
Andesitic volcanic rocks: Socal-Schroeder	2.57	Brocher and Ruebel (1998)	Well logs
Andesite – global average	5 to 25	Christensen and Mooney (1995)	Handsample

Basalt (Unaltered)

Data Source	Depth (km)	Reference	Data Type
Basalts	0.01-0.02	Boore (2003)	VSP
Crescent Fm.: OL-1, -7, -8, -14, -29	0.66	Brocher and Christensen (2001)	Handsample
Siletz River: Breccia: Harris #1-4	0.96	Brocher and Horta (1998)	Well logs
Crescent Fm.: Pope & Talbot #3-1	1.04	Brocher and Ruebel (1998)	Well logs
Crescent Fm. V: Pope & Talbot #18-1	1.13	Brocher and Ruebel (1998)	Well logs
Crescent Fm.?: Dungeness #1	1.50	Brocher and Ruebel (1998)	Well logs
Siletz River: Pillow Lava: Harris #1-4	1.52	Brocher and Horta (1998)	Well logs
Siletz River: Breccia: Sutherlin Unit #1	1.65	Brocher and Horta (1998)	Well logs
Siletz River: Breccia: Coos County #1	1.72	Brocher and Horta (1998)	Well logs
Crescent Fm.: Socal Whidbey	1.92	Brocher and Ruebel (1998)	Well logs
Siletz River: Pillow Lava: Coos County #1	1.97	Brocher and Horta (1998)	Well logs
Basalts: Silvana Community #12-1	2.24	Brocher and Ruebel (1998)	Well logs
Miocene volc.: Bethlehem #1	2.30	Brocher (2005b)	Well logs
Siletz River: Breccia: Weyerhaeuser B-1	2.31	Brocher and Horta (1998)	Well logs
Siletz River: Pillow Lava: Sutherlin Unit #1	2.31	Brocher and Horta (1998)	Well logs
Miocene volcanics: Bethlehem #2	2.80	Brocher (2005b)	Well logs
Siletz River: Pillow Lavas: Weyerhaeuser B-1	3.00	Brocher and Horta (1998)	Well logs
Miocene volcanic rocks: San Pablo Basin	3.20	Smith (1992), Wright and Smith (1992)	Well logs
Siletz River: Pillow Lavas: Sutherlin Unit #1	3.50	Brocher and Horta (1998)	Well logs
Basalt – global average	5 to 25	Christensen and Mooney (1995)	Handsample

Franciscan Complex (Metagraywacke)

Data Source	Depth (km)	Reference	Data Type
Franciscan sandstone: moderate weathering	0	Fumal (1978)	VSP
Franciscan sandstones and shales	0.01-0.05	Boore (2003)	VSP
Santa Clara Valley: GUAD borehole	0.40-0.41	Newhouse et al. (2004)	Suspension Log
Olympic Core Complex: OLG-1 to OLG-3, OLG-5 to OLG-12	0.66	Brocher and Christensen (2001)	Hand sample
Wisner Unit 1, #1: Livermore Valley	0.62-1.04	Brocher (2005b)	Well logs
Outer Santa Cruz Basin (#36)	2.70	Brocher (2005b)	Well logs
Franciscan graywacke	3.30	Stewart and Peselnick (1978);	Handsample
Franciscan shale	3.30	Stewart and Peselnick (1978);	Handsample
Franciscan sandstone	3.30	Stewart and Peselnick (1978);	Handsample
Loma Prieta metagraywacke	0.66 to 20	N. I Christensen (1997, writ. comm.)	Handsample
Franciscan melange	3.30	Stewart and Peselnick (1978); 1kbar	Handsample
Metagraywacke – global average	5 to 25	Christensen and Mooney (1995)	Handsample
Franciscan complex: Great Valley	0 to 20	Godfrey et al. (1997)	Gravity model
Franciscan complex: Great Valley	0 to 12	Griscom and Jachens (1990)	Gravity model
Franciscan complex: Clear Lake	0 to 15	Castillo and Ellsworth (1993)	EQ tomography
The Geysers	0-1.55	Majer et al. (1988)	VSP
Mendocino Triple Junction: Central and Eastern Belt Franciscan	0 to 5	Godfrey et al. (1997)	2D refraction tomo.
Mendocino Triple Junction: Central and Eastern Belt Franciscan	0 to 18	Beaudoin et al. (1996)	2D refraction tomo.
Franciscan: Marin Headland	0.9 to 2.5	Boatwright et al. (2004)	2D refraction tomo.

Franciscan: Marin Peninsula	2	Hole et al. (2000)	3D seismic tomo.
Franciscan: Diablo Range	0 to 15	Walter and Mooney (1982)	Seismic refraction
Franciscan: San Simeon	0 to 12	Hauksson et al. (2004)	3D seismic tomo.
Franciscan: Hayward fault	11 to 17	Hardebeck et al. (2004)	3D seismic tomo.
Franciscan complex: SF Peninsula	1 to 13	Parsons and Zoback (1997)	3D seismic tomo.

Gabbro

Data Source	Depth (km)	Reference	Data Type
Salinian Gabbro of Logan	6	Langenheim et al. (1997)	Gravity model
Metagabbro (greenschist facies)	3.3	Christensen (1978): 1 kbar	Handsample
Metagabbro (amphibolite facies)	3.3	Christensen (1978): 1 kbar	Handsample
Gabbro	3.3	Christensen (1978): 1 kbar	Handsample
Sierran affinity material	17.5	Griscom and Jachens (1990)	Gravity model
Gabbro-Norite-Troctolite – global average	5 to 25	Christensen and Mooney (1995)	Handsample
Great Valley Ophiolite	0 to 9.5	Griscom and Jachens (1990)	Gravity Model

Granites

Data Source	Depth (km)	Reference	Data Type
Cretaceous granitic rocks: soft (grus)	0	Fumal (1978)	VSP
Cretaceous granitic rocks: hard	0	Fumal (1978)	VSP
Gabilan Range: fractured Quartz diorite	0.0-0.6	Stierman and Kovach (1977)	Well Log
Granite	0.00-0.02	Boore (2003); Brocher's compilation	VSP
Granite: South Bay (USGS CB-1)	0.20	Brocher (2005b)	Well Log
Granite: Salinas Valley (Clark #1)	0.62	Brocher (2005b)	Well Log
Granite: Salinas Valley (Chesholm #1)	0.65	Brocher (2005b)	Well Log
Granite: Salinas Valley (Salinas Land #1)	0.69	Brocher (2005b)	Well Log
Granite: Bodega Basin (Offshore #41)	1.41	Brocher (2005b)	Well Log
Granite: Bodega Basin (Offshore #39)	1.70	Brocher (2005b)	Well Log
Granite?: Point Arenas Basin	1.92	Brocher (2005b)	Well Log
Salinian Granites (SAFOD Pilot Hole)	0.7-2.1	Boness and Zoback (2004)	Borehole log
Salinian Gabilan Range plutons	5	Jachens and Griscom (2004)	Gravity model
Salinian Ben Lomond Mtn pluton	5	Jachens and Griscom (2004)	Gravity model
Salinian Montara Mtn pluton	5	Jachens and Griscom (2004)	Gravity model
Loma Prieta granodiorite	0.66-20	N. I. Christensen (1997, writ. comm.)	Handsample
Eastern Great Valley basement	0.2	Zoback and Wentworth (1986)	Seismic refraction
Sierras: Lake Oroville: metamorphic belt	0	Spieth et al. (1981)	Seismic refraction
Sierran affinity material	0.2	Griscom and Jachens (1990)	Gravity model
Sierra Nevada Batholith	3 to 30	Fliedner et al. (2000)	3D refraction tomo.
Sierra Nevada tonalites SN-1, SN-2	5	Fliedner et al. (2000); room temp.	Handsample
Sierras: Lake Oroville: metamorphic belt	0.6	Spieth et al. (1981)	Seismic refraction
Eastern Great Valley basement	2.7	Zoback and Wentworth (1986)	Seismic refraction
Trondhjemite	3.3	Christensen (1978): 1 kbar	Handsample
Spilite	3.3	Christensen (1978): 1 kbar	Handsample
Granite-Granodiorite – global average	5 to 40	Christensen and Mooney (1995)	Handsample
Salinian granite: SF Peninsula	0 to 1.5	Parsons and Zoback (1997)	2D seismic tomo.

Greenstones

Data Source	Depth (km)	Reference	Data Type
Franciscan greenstone: moderate weathering	0.05	Fumal (1978)	VSP
Franciscan greenstone: fresh?	0.01	Boore (2003); Brocher's compilations	VSP
Franciscan greenstone: fresh	0.05	Fumal (1978)	VSP
Greenschist facies basalt – global average	5 to 25	Christensen and Mooney (1995)	Handsample

Meta Basalts

Rock Type	Depth (km)	Reference	Data Type
Zeolite Facies Basalt – global average	5 to 40	Christensen and Mooney (1995)	Handsample
Prehnite-Pumpelleyite Facies Basalt - global average	5 to 40	Christensen and Mooney (1995)	Handsample

Serpentinites

Data Source	Depth (km)	Reference	Data Type
Franciscan serpentine	0.02	Borcherdt and Glassmoyer (1992)	VSP
Serpentinite	0.01 to 0.08	Boore (2003)	VSP
Serpentinite	3.30	Christensen (1978): 1 kbar	Handsample
Loma Prieta serpentinite	0.66 to 20	N. I. Christensen (1997, writ. comm.)	Handsample
Serpentinite	5 to 30	Christensen and Mooney (1995)	Handsample

Miocene Tuffs (proxy for the Sonoma Volcanics)

Data Source	Depth (km)	Reference	Data Type
Yucca Mtn. Tuffs	0-3.6	Brocher et al. (1998)	Gravity model
UE-25 P-1	0.4-1.15	Brocher et al. (1996)	Borehole log
USW H-4	0.65-1.25	Brocher et al. (1996)	Borehole log
USW H-6	0.55-1.2	Brocher et al. (1996)	Borehole log
G1 and H1	0.4-1.83	Hoffman and Mooney (1984)	Borehole log
Crater Flat seismic lines	1.4-3.3	Mooney and Schapper (1995)	Seismic refraction

Vs as a function of Vp

One of the most important relationships summarized here is that between Vp and Vs. Most velocity models are derived in terms of the much more numerous Vp data, but strong ground motions are more nearly a function of Vs than Vp because shear and surface waves cause most of the damage (Joyner, 2000). For this reason, Vp models are then converted to Vs models. Brocher (2005a) recently reviewed existing Vs as a function of Vp relations, and proposed several new empirical relations based on a compilation of a wide-variety of common rock types. Many of these measurements were from northern California.

Figure 1 plots Vs versus Vp (from Brocher, 2005a), as well as Vp and Vs observations from seismic tomography along the Hayward fault (Hardebeck et al., 2004). Brocher (2005a) reported that a regression of Vp and Vs observations for all units except calcium rich rocks, mafic rocks (including gabbros), and serpentinites yielded the following new empirical relationship, called "Brocher's regression fit", between Vp and Vs:

[eqn. 1] $$\mathbf{Vs\ (km/s) = 0.7858 - 1.2344Vp + 0.7949Vp^2 - 0.1238Vp^3 + 0.0064Vp^4.}$$

Equation 1 is valid for $1.5 < Vp < 8$ km/s.

The data in Figure 1 are also consistent for compressional wave velocities between 1.5 and 4.5 km/s with a linear regression of borehole and VSP measurements for clay-rich sedimentary rocks, the so called "mudline", of Castagna et al. (1985):

[eqn. 2] $$\mathbf{Vs\ (km/s) = (Vp-1.36)/1.16.}$$

Vp as a function of Vs is often given as Poisson's ratio, which is simply a function of Vp/Vs containing no new information. Brocher (2005a) also proposed a new empirical relation for Poisson's ratio (σ) and Vp for Vp between 1.5 and 8.5 km/s:

[eqn. 3] $\sigma = 0.8835 - 0.315Vp + 0.0491Vp^2 - 0.0024Vp^3.$

Equation 3 excludes data for calcium-rich and mafic rocks. I refer to Equation 3 as "Brocher's empirical fit" to emphasize that the data were fit by eye.

Figure 1 shows another empirical relation derived from Ludwig et al. (1970), using their empirical Poisson's ratio versus σ and Vp versus σ relations (Brocher, 2005a). For Vp between 1.5 and 8.5 km/s, this relation is:

[eqn. 4] $\sigma = 0.769 - 0.226Vp + 0.0316Vp^2 - 0.0014Vp^3.$

Equation 4 is referred to as "Ludwig's empirical fit". The relations defined in "Brocher's empirical fit" (equation 3) and "Ludwig's empirical fit" are nearly identical, and deviate most for Vp between 3 and 6 km/s.

Vs predicted from Vp using "Brocher's regression fit", "Brocher's empirical fit" and "Ludwig's empirical fit" generally lie within 0.1 km/s of each other (Figure1). Vs values predicted by the "mudline" (Castagna et al., 1985), matches the data below Vp of 4.5 km/s. For Vp greater than 4.5 km/s, it over predicts Vs.

Vs values for calcium-rich rocks (including dolomites and anorthosites), mafic rocks, and gabbros lie 0.2 to 0.3 km/s below the general trend in Figure 1. For these units,

[eqn. 5] $Vs\ (km/s) = 2.88 + 0.52(Vp-5.25).$

better fits the observations for Vp between 5.25 and 7.25 km/s (Brocher, 2005a), and is called the "mafic line".

Among others, Christensen (1996) reported that serpentinites have anomalous Vp and Vs relations. For confining pressures of 200 MPa, he reported an average Vp of 5.31 km/s and an average Vs of 2.59 km/s for 30 samples from 10 different serpentinites. This average value plots about 0.5 km/s below the general trend in Figure 1.

Equations 1 to 4 represent a significant departure from the relations used in the 1997 USGS Velocity Model for the Bay Area (Brocher et al., 1997). Based on equations 1 to 4, the Vs used in the sedimentary basins by Brocher et al. (1997) was too low (by a factor of 30% or more). Subsequent observations of compressional wave arrival times from local and teleseismic earthquakes in Santa Clara Valley indicate that that the geometry of the Cenozoic basins and the Vp used in the basins there (Brocher et al., 1997) are accurate (Fletcher et al., 2003). Fletcher et al. (2003) and Boatwright et al. (2004) note, however, that Vs used in this model within the basins are too small. Using equations 1 or 2 to calculate Vs from Vp in the velocity model of Brocher et al. (1997) would substantially improve the accuracy of the 1997 model in these basins by increasing the model Vs in the basins. This increase in Vs, in turn, should decrease basin amplification effects in the USGS Bay Area Velocity Model 05.0.0 relative to those in the 1997 USGS Velocity Model.

Density as a function of Vp

For the USGS Bay Area Velocity Model 05.0.0 we calculated density from Vp. Figure 2 plots several proposed density (ρ) versus Vp relations. The filled circles on Figure 2 show values picked from the Nafe-Drake relation published by Ludwig et al. (1970) for a wide variety of sedimentary and crystalline rock types. The solid line shows a polynomial regression fit to these values, and because it consists of a single smooth curve valid for Vp between 1.5 and 8.5 km/s, it represents a very useful density versus Vp relation:

[eqn. 6] $\rho\ (g/cm^3) = 1.6612Vp - 0.4721Vp^2 + 0.0671Vp^3 - 0.0043Vp^4 + 0.000106Vp^5.$

Equation 6 is the "Nafe-Drake curve" (Ludwig et al., 1970).

Figure 2 compares the Nafe-Drake curve to Gardner's rule (Gardner et al., 1984) often used for sedimentary rocks and for compressional wave velocities between 1.5 and 6.1 km/s. Gardner's rule is the dashed line in Figure 2:

[eqn. 7] $\rho\ (g/cm^3) = 1.74Vp^{0.25}.$

Gardner's rule, defined for, yields ρ that are higher for all Vp, usually by less than 0.1 g/cm^3, than predicted by the Nafe-Drake curve. Gardner's rule most deviates from the Nafe-Drake curve for Vp less than 2 km/s, typical of Holocene and Plio-Quaternary sedimentary rocks and deposits.

Available comparisons suggest that for sedimentary rocks in Northern California Gardner's rule may be more accurate than the Nafe-Drake curve. On average, Gardner's rule more

accurately predicts the observed density log from the observed sonic logs in 26 oil industry boreholes for which both logs are available, and for which Vp generally exceeds 2 km/s (Brocher, 2005b). The most direct comparison is for 11 offshore boreholes where both logs were digitized at uniform intervals of 0.5 feet. For these 11 pairs of logs, the observed density logs were fit within 1% on average using the coincident sonic log to calculate Gardner's rule (Brocher, 2005b). On average, Gardner's rule also fit sonic and density log data from 15 onshore boreholes (Brocher, 2005b). Parsons et al. (2001) also show that sedimentary rocks within Puget Lowland and metagraywackes from the Olympic Peninsula, Washington, are well matched by Gardner's rule for Vp from 2 to 6 km/s.

Christensen and Mooney's (1995) widely-used ρ versus Vp relation for crystalline rocks (Vp between 5.5 and 7.5 km/s) is:

[eqn. 8] ρ **(g/cm^3) = 0.541 + 0.3601Vp.**

For Vp greater than 6 km/s, this relation (equation 8) predicts ρ up to 0.15 g/cm^3 greater than that by the Nafe-Drake curve. Figure 2 shows their relation for all rocks except volcanic and monomineralic rocks at 10 km depth from their Table 7.

Godfrey et al. (1997) proposed a separate ρ versus Vp relation for basalts, diabase, and gabbros for Vp between 5.9 and 7.1 km/s:

[eqn. 9] ρ **(g/cm^3) = 2.4372 + 0.0761Vp.**

Their relation (eqn. 9) deviates up to 0.2 g/cm^3 from the Nafe-Drake curve. Their relation is based on Christensen and Mooney's (1995) published values for basalts, diabase, and gabbros at 10 km depth. If values for zeolite, greenschist, and prehnite-pumpellyite facies basalts from Christensen and Mooney (1995) are combined with these values this relation yields slightly lower ρ for Vp between 5.9 and 7.1 km/s:

(eqn. 10) ρ **(g/cm^3) = 2.2428 + 0.1052Vp.**

Finally, Figure 2 plots the global average value for serpentinites at 10 km (Christensen and Mooney, 1995). This value plots directly on the Nafe-Drake curve, indicating that serpentinites have a standard ρ versus Vp relation.

Qs as a function of Vs

For computational convenience, we use the following Qs as a function of Vs relation to calculate Qs from the velocity model. This relation is largely derived from a comparison of observed and calculated seismic amplitudes for a 3D velocity model of the Los Angeles basin (Olsen et al., 2003). Olsen et al. (2003) showed that this relation approximates results from a number of previous studies of Qs. A separate constant for Qs is required for saltwater.

Qs = 10 for Vs (km/s) < 0.5 km/s (based on shallow borehole studies by Tullos and Reid (1969), Hamilton (1972), Gibbs et al. (1994), Liu et al. (1994), and Kudo and Shima (1970)). San Francisco Bay Area specific studies include Gibbs et al. (1994) and Liu et al. (1994).

Qs = 20Vs (km/s) for 0.5 km/s < Vs < 1.5 km/s (Olsen et al., 2003).

Qs = 100Vs (km/s) for Vs > 1.5 km/s (Olsen et al., 2003).

Qs = 40,000 for saltwater (Assumed).

Qp as a function of Qs

For computational convenience, we use the following Qp as a function of Qp relation to calculate Qp. This relation is largely derived from a comparison of observed and calculated seismic amplitudes for a 3D velocity model of the Los Angeles basin (Olsen et al., 2003). The seismic amplitudes, however, are less sensitive to Qp than to Qs, so this relation may be more approximate. A separate constant for Qp is required for saltwater.

Qp = 1.5Qs (Olsen et al., 2003).

Qp = 63,000 for saltwater (Johnston, 1981)

Andesites

This section is the first of several that discuss Vp as a function of depth for various rock types used in USGS Bay Area Velocity Model 05.0.0. Each section is organized similarly, having figures that illustrate the available data, and regressions to the data. Data sources are summarized in Table 1.

Figure 3A plots Vp versus depth for andesites. Sources of these data (Table 1) include a USGS 30-m VSP measurement for rhyolite (Fumal, 1978), a borehole sonic log from Puget Lowland, Washington that intersected andesitic rocks at 2.57 km depth (Socal Schroeder #1; Brocher and Ruebel, 1998), and global averages of tens of laboratory measurements of Vp at 5 km intervals for andesites (Christensen and Mooney, 1995). The Vp at z=0 km is assumed to be 2.5 km/s.

For depths between 0 and 7.5 km:

(eqn. 11) $\mathbf{Vp\ (km/s) = 2.5 + 0.8114z - 0.0746z^2 + 0.0029z^3 - 0.00004z^4,}$

for depths between 7.5 and 25 km use:

(eqn. 12) $\mathbf{Vp\ (km/s) = 5.5 + 0.0074\ (z-7.5).}$

As shown in Figure 3A, Equation 12 is constrained solely by laboratory measurements reported by Christensen and Mooney (1995).

For andesite, convert Vp to Vs following Brocher (2005a):

for Vp between 1.5 and 4.11 km/s use "Brocher's regression fit",

[1] $\mathbf{Vs\ (km/s) = 0.7858 - 1.2344Vp + 0.7949Vp^2 - 0.1238Vp^3 + 0.0064Vp^4,}$

for Vp greater than 4.11 km/s use the "mafic line":

[5] $\mathbf{Vs\ (km/s) = 2.88 + 0.52\ (Vp-5.25).}$

Basalts (Unaltered)

Figure 3B plots regressions of Vp versus depth data for unaltered basalts from sources summarized in Table 1. These data include averages of sonic logs for several oil industry boreholes from Oregon and Washington that intersect basaltic rocks (Crescent Formation or Siletz River basalts) at various depths up to 3 km (Brocher and Horta, 1998; Brocher and Ruebel, 1998), sonic logs of basalts in the San Pablo Bay (Smith, 1992; Wright and Smith, 1992; Brocher, 2005b), several laboratory measurements of basalts from the Crescent Formation in the Puget Lowland (Brocher and Christensen, 2001), and global averages of laboratory measurements of basalts at 5 km intervals up to 35 km (Christensen and Mooney, 1995). The Vp at z=0 km is assumed to be 3 km/s.

For depths between 0 and 4.3 km use:

(eqn. 13) Vp (km/s) = $3.0 + 1.1691z - 0.1523z^2 + 0.0089z^3 - 0.0002z^4 + 0.000002z^5$,

for depths between 4.3 and 25 km use:

(eqn. 14) Vp (km/s) = 5.85 + 0.0035 (z-4.3).

For unaltered basalts convert Vp to Vs following Brocher (2005a):

For Vp between 1.5 and 4.11 km/s use "Brocher's regression fit",

[1] Vs (km/s) = $0.7858 - 1.2344Vp + 0.7949Vp^2 - 0.1238Vp^3 + 0.0064Vp^4$,

for Vp greater than 4.11 km/s use the "mafic line":

[5] Vs (km/s) = 2.88 + 0.52 (Vp-5.25).

These relations are not valid for volcanic breccias, whose Vp are about 1 km/s lower than those predicted here (Brocher and Horta, 1998).

Franciscan Complex (Metagraywacke)

Table 1 and Figure 4A summarize the large number of sources available for metagraywackes and the Franciscan Complex. Metagraywacke is the dominant lithology within the Franciscan Complex (Thompson and Talwani, 1964). To investigate the Vp of the Franciscan Complex near the surface, I compiled USGS 30-m VSP data that intersect Franciscan Complex at or near the surface (Boore, 2003). A linear regression of these data, fixing the intercept at 0.7 km/s, yielded Vp (km/s) = 0.7 + 52.4z, $0 < z < 0.05$ km. However, this relation over predicts Vp at 0.05 km depth and so I propose a relation that matches the VSP data for Tertiary sedimentary rocks (Figure 9B).

For depths between 0 and 0.05 km:

(eqn. 15) $\mathbf{Vp\ (km/s) = 0.7 + 36z.}$

Equation 15 yields Vp of 2.5 km/s at 50 m depth (Figure 9B), in agreement with Equation 16. Note that the value (0.7 km/s), for z=0 km, is assumed.

To derive a relation below 50 m, I compiled VSP and sonic log data for the Franciscan Complex at various depths up to 2.7 km (Majer et al., 1988; Newhouse et al., 2004; Brocher, 2005b), laboratory measurements of Franciscan Complex rocks (Stewart and Peselnick, 1978), laboratory measurements for graywackes (Christensen and Mooney, 1995; Brocher and Christensen, 2001), and tomography velocities at various depths up to 20 km (Beaudoin et al., 1996; Parsons and Zoback, 1997; Hole et al., 2000; Boatwright et al., 2004; Haukkson et al., 2004; Hardebeck et al., 2004). These observations (Figure 4A) were fit with a 5th order polynomial:

For depths between 0.05 and 9 km use:

(eqn. 16) $\mathbf{Vp\ (km/s) = 2.5 + 1.963z - 0.424z^2 + 0.043z^3 - 0.002z^4 + 0.0000335z^5,}$

for depths between 9 and 25 km use:

(eqn. 17) **$Vp\ (km/s) = 6.00 + 0.01\ (z-9).$**

Below 5 km, tomography measurements of Vp are approximately 0.5 km/s higher than laboratory measurements (Christensen and Mooney, 1995) (Figure 4A), perhaps indicative of a significant greenstone component in the Franciscan Complex.

Table 2 represents an attempt to predict the spatial variability expected for Franciscan metagraywacke units based on their estimated average densities (R. C. Jachens, writ. comm., 2005). These units correspond to separate blocks of Franciscan Complex defined in the USGS Bay Area Velocity Model 05.0.0. Assuming a global average density for the Franciscan metagraywackes of 2.67 g/cm^3 (Jachens and Griscom, 2004), I calculated the expected velocity perturbation of each block using relations published in Christensen and Mooney (1995). Using these relations the small density differences in Table 2 yield small velocity perturbations between –0.04 and 0.13 km/s.

For Franciscan Complex rocks (metagraywacke), convert Vp to Vs using "Brocher's regression fit" (Brocher, 2005a):

[1] **$Vs\ (km/s) = 0.7858 - 1.2344Vp + 0.7949Vp^2 - 0.1238Vp^3 + 0.0064Vp^4.$**

Table 2. Variations in the Vp of blocks within the Franciscan Complex based on their average density relative to a global average density of 2.67 g/cm^3 for Franciscan Complex (densities reported by R. C. Jachens, writ. comm., 2005).

No volcs Vp km/s	All rocks Vp km/s	Diff. km/s	Average Density g/cm^3	Franciscan block location
5.941	5.848	0.03	2.680	Alexander
5.913	5.814	0.00	2.670	Berkeley
5.941	5.848	0.03	2.680	Central Bay
5.886	5.779	-0.03	2.660	Diablo Range East
5.872	5.762	-0.04	2.655	Diablo Range West
5.872	5.762	-0.04	2.655	Evergreen

6.024	5.952	0.11	2.710	Foothills
5.941	5.848	0.03	2.680	Gabilan
6.038	5.969	0.13	2.715	Halfmoon Bay
5.941	5.848	0.03	2.680	Merced
5.955	5.865	0.04	2.685	Napa
5.913	5.814	0.00	2.670	North Coast
6.038	5.969	0.13	2.715	Pilarcitos
5.886	5.779	-0.03	2.660	San Felipe
5.997	5.917	0.08	2.700	San Leandro
5.886	5.779	-0.03	2.660	South Coast
5.941	5.848	0.03	2.680	Santa Rosa
5.955	5.865	0.04	2.685	Sonoma

Velocities in the first two columns are calculated from Table 7 of Christensen and Mooney (1995) at 10 km: the first column is for the relation that includes no volcanics and the second column is for the relation that includes all rocks. The velocity difference shown in the third column is that calculated using the first column and the Vp (5.99 km/s) calculated using the global average density for the Franciscan Complex of 2.67 g/cm^3 (and the no volcanics equation of Christensen and Mooney (1995)).

Gabbros

Figure 4B and Table 1 summarize the limited data available for gabbros. These include those calculated from gravity models (Griscom and Jachens, 1990; Langenheim et al., 1997; Jachens and Griscom, 2004), laboratory measurements of gabbros (Christensen, 1978), and global averages of laboratory measurements of gabbros at 5 km intervals up to 35 km (Christensen and Mooney, 1995). There are no USGS 30-m VSP data for gabbros. The Vp at z=0 km is assumed to be 3 km/s. For simplicity, I fit the limited data with two linear velocity gradients rather than a smoothly varying curve (Figure 4B).

For depths between 0 and 2 km, use:

(eqn. 18) $\mathbf{Vp\ (km/s) = 3.0 + 2z,}$

and for depths between 2 and 25 km:

(eqn. 19) $\mathbf{Vp\ (km/s) = 7.0 + 0.002\ (z-2).}$

For gabbro, convert Vp to Vs following Brocher (2005a):

For Vp between 1.5 and 4.11 km/s use "Brocher's regression fit",

[1] $\mathbf{Vs\ (km/s) = 0.7858 - 1.2344Vp + 0.7949Vp^2 - 0.1238Vp^3 + 0.0064Vp^4,}$

for Vp greater than 4.11 km/s use the "mafic line":

[5] $\mathbf{Vs\ (km/s) = 2.88 + 0.52\ (Vp-5.25).}$

Granites

A large suite of data, summarized in Table 1 and plotted in Figure 5, are available to constrain Vp versus depth for Salinian and Sierran granites. Figures 5A and 5B compile well log data that intersect Salinian and Sierran granites at various depths up to 2.1 km (Stierman and Kovach, 1979; Boness and Zoback, 2004; Brocher, 2005b), density models (Jachens and Griscom, 2004), laboratory measurements of granitic rocks (Christensen, 1978; Fliedner et al., 2000), and refraction and tomography velocities at various depths up to 35 km (Zoback and Wentworth, 1986; Spieth et al., 1981; Fliedner et al., 2000).

Assuming the Vp at z=0 km is 1.5 km/s, the USGS "30-m" borehole VSP data (Boore, 2003) and sonic logs of granitic rocks in shallow boreholes (Brocher, 2005b) plotted in Figure 5B yields:

For depths between 0 and 0.5 km:

(eqn. 20) $\mathbf{Vp\ (km/s) = 1.5 + 4.41z}$

for depths between 0.5 and 4 km,

(eqn. 21) $\mathbf{Vp\ (km/s) = 2.5 + 2.9299z - 0.824z^2 + 0.1019z^3 - 0.0061z^4 + 0.0002z^5,}$

for depths between 4 and 25 km:

(eqn. 22) $\mathbf{Vp\ (km/s) = 6.20 + 0.002\ (z-4).}$

Figure 5B shows that equation 22 is based on data from Christensen and Mooney (1995), N. I. Christensen (writ. comm., 1997), and Fliedner et al., (2000).

For granite, convert Vp to Vs using "Brocher's regression fit" (Brocher, 2005a):

[1] $\mathbf{Vs\ (km/s) = 0.7858 - 1.2344Vp + 0.7949Vp^2 - 0.1238Vp^3 + 0.0064Vp^4.}$

Great Valley Sequence

The Jurassic and Cretaceous Great Valley Sequence of sedimentary rocks is largely confined to the Great Valley, West Delta, Livermore Valley, and east of the Hayward and Calaveras faults (Figure 6). The Vp versus depth relation in the Great Valley Sequence is largely constrained by sonic well log data from tens of oil industry boreholes up to 6 km deep (Brocher, 2005b). Most boreholes sample depths no more than 3 or 4 km. Figure 7 plots many of these borehole logs (as well as for other Tertiary rocks) and shows a linear regression to these data (equations 23 and 24).

Figure 8A shows that at greater depths the Vp versus depth relation is constrained by seismic refraction studies in the Great Valley and Livermore Valley (Colburn and Mooney, 1986; Holbrook and Mooney, 1987; Meltzer et al., 1987; MacGregor-Scott and Walter, 1988; Godfrey et al., 1997) and seismic tomography models (Hole et al., 2000; Hardebeck et al., 2004). Meltzer et al. (1987) and MacGregor-Scott and Walter (1988) report a velocity of about 5.5 km/s at the top of the Great Valley sequence at a depth of about 5 km. Hardebeck et al (2005) report a Vp of about 5.5 km/s at a depth of 7 km. Equations 23 to 25 approximate these measurements (Figure 8A):

For depths between 0.05 and 4 km, use:

(eqn. 23) $\mathbf{Vp\ (km/s) = 2.24 + 0.6z,}$

for depths between 4 and 7 km, use:

(eqn. 24) $\mathbf{Vp\ (km/s) = 4.64 + 0.3*(z - 4),}$

for depths between 7 and 25 km, use:

(eqn. 25) $\mathbf{Vp\ (km/s) = 5.54 + 0.06*(z-5).}$

For the Great Valley Sequence, convert Vp to Vs using "Brocher's regression fit" (Brocher, 2005a):

[1] $\mathbf{Vs\ (km/s) = 0.7858 - 1.2344Vp + 0.7949Vp^2 - 0.1238Vp^3 + 0.0064Vp^4.}$

Greenstones/Greenschist Facies Basalts

Figure 8B and Table 1 summarize the rather sparse data available for greenschist facies basalts. Greenstones and unaltered basalts have different Vp versus Vs relations and thus greenstones are discussed separately here. I compiled three 30-m USGS borehole VSP observations for Franciscan greenstones (Fumal, 1978; Boore, 2003; T. M. Brocher, unpublished compilation), and laboratory measurements of greenschist facies basalts at 5 km intervals up to 35 km (Christensen and Mooney, 1995). Vp at z=0 km is assumed to be 3 km/s.

For depths between 0 and 5 km, use:

(eqn. 26) $$\mathbf{Vp\ (km/s) = 3.0 + 1.3229z - 0.1542z^2 + 0.0073z^3 - 0.0001z^4,}$$

and for depths between 5 and 25 km, use

(eqn. 27) $$\mathbf{Vp\ (km/s) = 6.65 + 0.006\ (z\text{-}5).}$$

For greenschist facies basalts, convert Vp to Vs using "Brocher's regression fit" (Brocher, 2005a):

[1] $$\mathbf{Vs\ (km/s) = 0.7858 - 1.2344Vp + 0.7949Vp^2 - 0.1238Vp^3 + 0.0064Vp^4.}$$

Unlike unaltered basalts, greenschist facies basalt fall on "Brocher's regression fit" given by Brocher (2005a), not the "mafic line".

Holocene Deposits

Vp and Vs for Holocene deposits (Table 3) are compiled from hundreds of published VSP measurements in the Bay Area (e.g., Fumal, 1978; Borcherdt and Glassmoyer, 1992; Boore, 2003). I have compiled these measurements into averages for different types of deposits (e.g., artificial fill, Holocene Bay Mud, Holocene fine-grained alluvium, Holocene medium-grained alluvium, Holocene coarse-grained alluvium) as a function of average depth of burial. For each unit Table 3 provides the number of samples averaged (N), the average depth of the measurement, and the average density, Vp, Vs, and Vp/Vs ratio. Vp/Vs ranges from 10.68 for artificial fill to 1.41 for Holocene coarse-grained alluvium. These Vp are plotted versus depth in Figure 11A. For the numerical relations please see equation 42 in the section on Plio-Quaternary deposits.

Table 3: Compilation of USGS 30-m borehole data for Holocene units in the Bay Area

Lithology	Depth (km)	Density (g/cm^3)	N	Vp (km/s)	N	Vs (km/s)	N	Vp/ Vs
Artificial fill (Qaf)	0.002	2.07	1	0.456	20	0.21	22	2.18
Artificial fill (Qaf)	0.006			1.186	5	0.13	5	8.98
Artificial fill (Qaf)	0.010			1.581	2	0.15	2	10.68
Holocene Bay Mud (Qhbm)	0.008	1.73	4	1.007	22	0.13	22	7.87
Holocene Bay Mud (Qhbm)	0.018			1.224	5	0.19	5	6.58
Holocene Bay Mud (Qhbm)	0.026			1.491	1	0.19	1	7.73
Holocene fine-grained alluvium (Qyf)	0.003	2.04	2	0.747	12	0.19	12	3.89
Holocene fine-grained alluvium (Qyf)	0.012	1.85	1	1.190	6	0.29	6	4.15
Holocene medium-grained alluvium (Qym)	0.002	1.82	1	0.390	11	0.19	11	2.02
Holocene medium-grained alluvium (Qym)	0.008	1.88	3	1.280	12	0.25	12	5.12
Holocene medium-grained alluvium (Qym)	0.016	1.94	1	1.585	5	0.24	5	6.50
Holocene medium-grained alluvium (Qym)	0.030			1.660	2	0.32	2	5.20
Holocene medium-grained alluvium (Qym)	0.050			1.700	1	0.31	1	5.48
Holocene coarse-grained alluvium (Qyc)	0.001	2.1	1	0.357	1	0.25	1	1.41
Holocene coarse-grained alluvium (Qyc)	0.005			0.952	2	0.35	2	2.71
Holocene coarse-grained alluvium (Qyc)	0.015	2.24	1	1.430	2	0.48	2	3.00
Holocene coarse-grained alluvium (Qyc)	0.028			1.995	1	0.73	1	2.74

Note: Abbreviations to units are from various USGS Open-File reports referenced by Boore (2003).

La Honda Basin

The La Honda basin is an elongate trough subparallel to and lying west of the San Andreas fault (Figure 6). The Cenozoic basin fill in the La Honda basin has an unusually high Vp compared to other sedimentary basins (Figure 9), and for this reason I discuss it separately from other older Cenozoic sedimentary rocks. It is important to note, however, that equations 28 and 29 discussed below were not used in the USGS Bay Area Velocity Model 05.0.0 because they are based solely on a gravity model. Equations 38 to 40, based on a great deal of sonic log data, were used to model sedimentary rocks in the La Honda basin.

To estimate the velocity-depth relation within the La Honda basin I converted three density-depth models used by Jachens and Griscom (2004) to velocity-depth functions using the Nafe-Drake curve (eqn. 6). Regression of data for the three density profiles (M-M', Q-Q', and S-S' from Jachens and Griscom (2004)), assuming an intercept value of 2.24 km/s (z=0 km), yields:

for depths between 0 and 3 km, use:

(eqn. 28) $\mathbf{Vp\ (km/s) = 2.24 + 2.62z - 0.7443z^2 + 0.0707z^3,}$

for depths between 3 and 6 km, use:

(eqn. 29) $\mathbf{Vp\ (km/s) = 5.32 + 0.027(z-3).}$

Equations 28 and 29 are nearly identical to those for Franciscan rocks (eqn. 16) to 2 km depth, and are about 0.5 km/s lower beginning at a depth of 3 km.

For the sedimentary rocks within the La Honda basin, convert Vp to Vs using "Brocher's regression fit" (Brocher, 2005a):

[1] $\mathbf{Vs\ (km/s) = 0.7858 - 1.2344Vp + 0.7949Vp^2 - 0.1238Vp^3 + 0.0064Vp^4.}$

Compilation of Vp and Vs for Tertiary sedimentary rocks in other sedimentary basins measured in USGS 30-m VSPs (Boore, 2003), suggests that equation 28 over predicts Vp in the upper 50 m. These VSP data are well matched by equation 15 (Figure 9B), but for depths between 0 and 0.05 km, can be approximated by:

(eqn. 30) **$Vp\ (km/s) = 0.7 + 31.4z.$**

Equation 30 predicts a Vp = 2.27 km/s at z = 0.05 km depth, which better matches the Vp predicted by equation 28 at this depth than equation 15.

At depths up to 0.05 km, I approximate Vs as a function of depth with two curves. First, based on the USGS 30-m VSP data for Tertiary sedimentary rocks in the Bay Area (Figure 9B) in the upper 0.037 km I use:

(eqn. 31) **$Vs\ (km/s) = 0.2149 + 18.3z - 138.1z^2.$**

For depths greater 0.037 km, I use the "mudline" (Castagna et al., 1985), to calculate Vs from equation 30:

[2] **$Vs\ (km/s) = (Vp - 1.36)/1.16.$**

Meta Basalts (Zeolite or Prehnite-pumpellyite Facies)

Christensen and Mooney's (1995) compilation of global laboratory Vp measurements indicates that zeolite and prehnite-pumpellyite facies basalts have different Vp versus depth relationships at depths greater than 5 km than either greenstones or unaltered basalts. In addition, the Vp for zeolite and prehnite-pumpellyite facies basalts (labeled meta basalt in Figure 3B) are about 0.5 km/s higher than those for unaltered basalts. For these reasons, I discuss them separately here. Based on Figure 3B I propose, however, to use the same relation as for unaltered basalts for the upper 5 km:

For depths between 0 and 5 km, use:

(eqn. 32) $\mathbf{Vp\ (km/s) = 3.0 + 1.1691z - 0.1523z^2 + 0.0089z^3 - 0.0002z^4 + 0.000002z^5,}$

for depths between 5 and 10 km, use:

(eqn. 33) $\mathbf{Vp\ (km/s) = 6.03 + 0.056\ (z-5),}$

for depths between 10 and 25 km, use:

(eqn. 34) $\mathbf{Vp\ (km/s) = 6.31 + 0.002\ (z-10).}$

For zeolite and prehnite-pumpellyite facies basalts, convert Vp to Vs using Brocher (2005a):

For Vp between 1.5 and 4.11 km/s, use "Brocher's regression fit" (Brocher, 2005a):

[1] $\mathbf{Vs\ (km/s) = 0.7858 - 1.2344Vp + 0.7949Vp^2 - 0.1238Vp^3 + 0.0064Vp^4,}$

for Vp greater than 4.11 km/s, use the "mafic line",

[5] $\mathbf{Vs\ (km/s) = 2.88 + 0.52\ (Vp-5.25).}$

Older Cenozoic Sedimentary Deposits

The following rules are based on Brocher's (2005b) compilation of sonic logs in oil industry boreholes for the upper 4 km. These basins, whose locations are shown in Figure 6, have slightly different velocity depth relationships that are summarized in Figure 10.

The three linear velocity gradients in equations 35 to 37 (identical to equations 23 to 25, and based on Figure 7) are useful in several basins (including the Great Valley, West Delta, and Livermore Valley). These relations are:

for depths between 0.05 and 4 km, use:

(eqn. 35) $\mathbf{Vp\ (km/s) = 2.24 + 0.6z,}$

for depths between 4 and 7 km, use:

(eqn. 36) $\mathbf{Vp\ (km/s) = 4.64 + 0.3*(z - 4),}$

for depths between 7 and 12 km, use:

(eqn. 37) $\mathbf{Vp\ (km/s) = 5.54 + 0.06*(z-5).}$

Equations 38 and 39 provide slightly more accurate fits to borehole data from Miocene transtensional basins (Salinas Basin and offshore basins (Figure 6)) and miscellaneous basins between the San Andreas and Hayward/Rodgers Creek faults (East Bay Trough) (Figure 10):

For depths between 0.05 and 4 km, use:

(eqn. 38) $\mathbf{Vp\ (km/s) = 2.314 + 0.35z + 0.2z^2 - 0.03z^3,}$

for depths between 4 and 7 km, use:

(eqn. 39) $\mathbf{Vp\ (km/s) = 4.99 + 0.04*(z-4).}$

The reduced velocity gradients at depths between 5 to 12 km (Figure 8A) are chosen to insure that the Vp for Great Valley Sequence at a depth of 7 km is about 5.5 km/s and increases to

about 5.8 km/s at 10 km depth (Meltzer et al., 1987; Colburn and Mooney, 1987; MacGregor-Scott and Walter, 1988; Hardebeck et al., 2004). Densities in the range of 2.55 to 2.61 g/cm^3 at about 10 km in the Great Valley (Griscom and Jachens, 1990; Godfrey et al., 1997) are consistent with a Vp between 5.13 and 5.45 km/s (Brocher, 2005a).

For all basins, convert Vp to Vs using "Brocher's regression fit" (Brocher, 2005a):

[1] $$\mathbf{Vs\ (km/s) = 0.7858 - 1.2344Vp + 0.7949Vp^2 - 0.1238Vp^3 + 0.0064Vp^4.}$$

My compilation of Vp and Vs for Tertiary sedimentary rocks measured in 30-m VSP's, compiled by Boore (2003), is plotted in Figure 9B as a function of depth. These data suggest that equations 35 and 38 significantly over predict Vp in the upper 0.05 km. Equation 30 provides an improved fit to these data to depths up to 0.05 km:

(eqn. 30) $$\mathbf{Vp\ (km/s) = 0.7 + 31.4z.}$$

Equation 30 predicts a Vp = 2.27 km/s at z = 0.05 km depth (Figure 9B), to match equations 35 and 38 at this depth.

At depths up to 0.037 km, I approximate Vs with:

(eqn. 31) $$\mathbf{Vs\ (km/s) = 0.2149 + 18.3z - 138.1z^2,}$$

see Figure 9B, and for depths greater than 0.037 km, I use the "mudline" (Castagna et al., 1985) to calculate Vs from equation 30:

[2] $$\mathbf{Vs\ (km/s) = (Vp - 1.36)/1.16.}$$

Plio-Quaternary Deposits

Plio-Quaternary deposits in Table 4 are assigned a Vp and Vs as a function of depth determined from my own compilation of published sources of USGS 30-m VSP measurements in the Bay Area (e.g., Fumal, 1978; Borcherdt and Glassmoyer, 1992; Boore, 2003). Polynomial regression of these VSP data as well as the VSP data for Holocene units in Table 3 (Figure 9B) yields, for depths between 0 and 0.04 km:

(eqn. 40) $\mathbf{Vp\ (km/s) = 0.536 + 56.008z - 661.9z^2,}$

(eqn. 41) $\mathbf{Vs\ (km/s) = 0.215 + 10.932z - 138.1z^2\ .}$

The primary application of these relations is for unsaturated deposits.

If instead the Vp at the surface is fixed at 0.7 km/s, then polynomial regression of these same data (Figure 11A), for depths between 0 and 0.04 km, yields:

(eqn. 42) $\mathbf{Vp\ (km/s) = 0.7 + 42.968z - 575.8z^2 + 2931.6z^3 - 3977.6z^4.}$

This latter relation better fits Vp in the upper 40-m of the boreholes logged in the Santa Clara Valley (STGA, STPK, MCGY, CCOC; Figure 12; Newhouse et al, 2004). Equation 42 should be used for the upper 0.04 km of the model for all mapped Holocene and Plio-Quaternary sedimentary deposits. At these shallow depths, Vs may be approximated by two linear gradients. For depths up to 0.037 km, use equation 41. For depths greater than 0.037 km, use the "mudline" (Castagna et al., 1985) to calculate Vs from equations 42 and 43:

[2] $\mathbf{Vs\ (km/s) = (Vp - 1.36)/1.16.}$

For greater depths, I regressed the average Vp in eleven borehole suspension and sonic logs from Santa Clara Valley (Figure 12, Newhouse et al., 2004), and plotted the value at the midpoint of

the log. Figures 11A and 11B also included values from USGS 30 m VSP data reported by Fumal (1978) and Borcherdt and Glassmoyer (1992).

For depths between 0.04 and 0.5 km use:

(eqn. 43) $\mathbf{Vp\ (km/s) = 1.5 + 3.735z - 3.543z^2,}$

for depths between 0.5 and 2 km use:

(eqn. 35) $\mathbf{Vp\ (km/s) = 2.24 + 0.6z.}$

Equations 43 assumes that the Plio-Quaternary deposits are water saturated such that its Vp at the surface is 1.5 km/s. Comparison of equations 42 and 43 to the sonic logs from Santa Clara Valley (Newhouse et al., 2004) yielded close fits (Figure 13) and are much more accurate than relations used by Brocher et al. (1997).

For Plio-Quaternary deposits having Vp greater than 1.5 km/s, calculate Vs using the "mudline" (Castagna et al., 1985):

[2] $\mathbf{Vs\ (km/s) = (Vp - 1.36)/1.16.}$

Table 4: Compilation of USGS 30-m borehole data for Plio-Quaternary units in the Bay Area

Lithology	**Depth (km)**	**Density (g/cm^3)**	**N**	**Vp (km/s)**	**N**	**Vs (km/s)**	**N**	**Vp/ Vs**
Dune Sand (Qyd)	0.003	2.11	2	0.818	5	0.23	5	3.53
Dune Sand (Qyd)	0.025	2.11	2	1.343	4	0.36	4	3.69
Dune Sand (Qyd)	0.027			1.610	1	0.46	1	3.52
Late Pleistocene fine-grained alluv. (Qof)	0.015	1.98	1	0.586	5	0.21	5	2.76
Late Pleistocene fine-grained alluv. (Qof)	0.020	1.99	3	1.351	26	0.27	26	4.99
Late Pleistocene fine-grained alluv. (Qof)	0.045	1.89	4	1.662	16	0.32	16	5.24
Late Pleistocene fine-grained alluv. (Qof)	0.057	1.95	2	1.624	8	0.36	8	4.54
Late Pleistocene fine-grained alluv. (Qof)	0.065			1.775	2	0.46	2	3.88
Late Pleistocene fine-grained alluv. (Qof)	0.074			1.775	2	0.43	2	4.16
Late Pleistocene med.-grained alluv. (Qom)	0.011	1.78	1	0.514	4	0.29	4	1.79

Late Pleistocene med.-grained alluv. (Qom)	0.029	1.97	7	1.516	30	0.37	30	4.12
Late Pleistocene med.-grained alluv. (Qom)	0.020			1.605	10	0.36	10	4.43
Late Pleistocene med.-grained alluv. (Qom)	0.052			1.643	4	0.59	4	2.81
Late Pleistocene med.-grained alluv. (Qom)	0.064			1.683	2	0.38	2	4.49
Late Pleistocene med.-grained alluv. (Qom)	0.075			1.837	1	0.41	1	4.45
Late-Pleistocene coarse-grained alluv. (Qoc)	0.041			1.377	10	0.52	10	2.66
Late-Pleistocene coarse-grained alluv. (Qoc)	0.053			1.632	3	0.54	3	3.01
Late-Pleistocene coarse-grained alluv. (Qoc)	0.061			0.959	1	0.61	1	1.57
Colma Fm. (Qc)	0.006	2.04	1	0.770	2	0.34	2	2.25
Colma Fm. (Qc)	0.015			1.091	3	0.28	3	3.92
Colma Fm. (Qc)	0.026			1.547	4	0.50	4	3.08
Colma Fm. (Qc)	0.048			1.725	1	0.42	1	4.14
Colma Fm. (Qc)	0.074			1.905	1	0.56	1	3.40
Colma Fm. (Qc)	0.099			1.831	1	0.56	1	3.25
Colma Fm. (Qc)	0.122			1.900	1	0.61	1	3.09
Santa Clara Formation (Qts)	0.006	2.18	2	0.315	3	0.21	3	1.48
Santa Clara Formation (Qts)	0.018	2.18	2	1.545	11	0.54	11	2.86
Santa Clara Formation (Qts)	0.029	2.18	2	1.929	9	0.59	9	3.30
Santa Clara Formation (Qts)	0.042	2.37	2	2.096	4	0.74	4	2.84
Santa Clara Formation (Qts)	0.065			2.089	1	0.52	1	4.02
Merritt Sand (Qm)	0.003			0.355	1	0.25	1	1.42
Merritt Sand (Qm)	0.011	1.99	1	1.371	4	0.36	4	3.80
Merritt Sand (Qm)	0.018	2.02	1	1.638	4	0.31	4	5.28
Merritt Sand (Qm)	0.024			0.986	1	0.43	1	2.30
Merritt Sand (Qm)	0.030			1.610	1	0.31	1	5.21
Merritt Sand (Qm)	0.037			1.610	1	0.53	1	3.06
Merced Formation (QTm)	0.003			0.249	3	0.14	3	1.79
Merced Formation (QTm)	0.012	2.00	2	1.083	4	0.34	4	3.22
Merced Formation (QTm)	0.021	2.05	1	1.210	3	0.36	3	3.32
Merced Formation (QTm)	0.030	2.05	1	1.450	2	0.43	2	3.39
Merced Formation (QTm)	0.141			1.811	2	0.77	2	2.36
Pleistocene Bay Mud (Older Bay Mud) (Qbm)	0.030	1.92	2	1.650	16	0.24	16	6.79
Pleistocene Bay Mud (Older Bay Mud) (Qbm)	0.052			1.766	13	0.33	13	5.32
Pleistocene Bay Mud (Older Bay Mud) (Qbm)	0.075			1.744	7	0.36	7	4.80
Pleistocene Bay Mud (Older Bay Mud) (Qbm)	0.094			1.754	3	0.39	3	4.49
Pleistocene Bay Mud (Older Bay Mud) (Qbm)	0.112			1.993	3	0.48	3	4.19

Serpentinites

The moderate amount of data for serpentinites is plotted in Figure 14A. These include values derived from USGS 30-m VSPs (Borcherdt and Glassmoyer, 1992; Boore, 2003; T. M. Brocher, unpub. compilation), laboratory measurements of serpentinites (Christensen, 1978; N. I. Christensen, writ. commun., 1997), and global averages of laboratory measurements of serpentinites at 5 km intervals up to 35 km depth (Christensen and Mooney, 1995). The Vp at z=0 km is assumed to be 2.3 km/s, in reasonable agreement with the USGS 30-m VSP data (Borcherdt and Glassmoyer, 1992; Boore, 2003; T. M. Brocher, unpub. compilation).

For depths between 0 and 2.56 km, use:

(eqn. 44) $\mathbf{Vp\ (km/s) = 2.3 + 1.9378z - 0.3701z^2 + 0.0294z^3 - 0.001z^4 + 0.00001z^5,}$

for depths between 2.56 and 25 km, use:

(eqn. 45) $\mathbf{Vp\ (km/s) = 5.29\ km/s.}$

For serpentinites, convert Vp to Vs for all Vp using:

(eqn. 46) $\mathbf{Vs = Vp/2.05}$

based on a global average for serpentinite data published by Christensen (1996).

The Vp and Vs of serpentinites are anomalously low for crystalline rocks (Figure 15). Christensen (1996), among many others, have noted this fact previously. Given their high magnetization (Saad, 1969), serpentinites are readily detectable in the subsurface using seismic refraction and aeromagnetic data (Blakely et al., 2005).

Sonoma Volcanics

I could locate no data for Miocene to Pliocene Sonoma Volcanics. Lacking data from the Sonoma Volcanics itself, as a proxy I compiled data for welded and nonwelded Miocene tuffs from the vicinity of Yucca Mountain, Nevada (Figure 14B). Although the Sonoma Volcanics are much more heterogeneous in composition and texture than Miocene tuffs from Yucca Mountain, there have been many more studies of the Vp and Vs of the latter tuffs than the former. Figure 14B shows values for these tuffs derived from several USGS sonic logs from the vicinity of Yucca Mountain (Hoffman and Mooney, 1984; Brocher et al., 1996), a density model for Crater Flat (Brocher et al., 1998), and laboratory measurements on tuffs recovered from boreholes (Martin et al., 1994; Price et al., 1994). Rather than showing the scattered well log data in Figure 14B, I have plotted regressions to these well log data. The Vp at z=0 km was assumed to be 1.5 km/s (Figure 14B).

For depths between 0 and 1.5 km, use:

(eqn. 47) $\mathbf{Vp\ (km/s) = 1.50 + 3.9236z - 1.778z^2 + 0.2607z^3,}$

for depths between 1.5 and 6 km, use:

(eqn. 48) $\mathbf{Vp\ (km/s) = 4.26 + 0.17(z-1.5).}$

Equation 48 is derived from seismic refraction models published by Mooney and Schapper (1995).

For the Sonoma Volcanics, convert Vp to Vs using "Brocher's regression fit" (Brocher, 2005a):

[1] $\mathbf{Vs\ (km/s) = 0.7858 - 1.2344Vp + 0.7949Vp^2 - 0.1238Vp^3 + 0.0064Vp^4.}$

Upper Mantle

For the upper mantle, assume the following constant values:

(eqn. 51) Vp (km/s) = 7.97 (Oppenheimer and Eaton, 1984), Vs (km/s) = 4.51 (Levander and Kovach, 1990), ρ (kg/m^3) = 3350 (assumed).

The upper mantle Vs, 4.51 km/s, is slightly lower than the value (4.59 km/s) predicted by equation 1 from the P-wave velocity. The assumed density, 3350 kg/m^3, lies between the values predicted by equations 6 and 8, 3280 kg/m^3 and 3411 kg/m^3, respectively.

Mafic Lower Crust

For the mafic lower crust, having velocities of 6.5 km/s and higher, assume the following constant values:

(eqn. 52) Vp (km/s) = 6.90 (Brocher et al., 1994; Holbrook et al., 1996), Vs (km/s) = 3.69 or 4.0 (Brocher et al., 1999), ρ (kg/m^3) = 3000 (assumed).

The lower crustal Vs for serpentinized mafic rocks, 3.69 km/s, is lower than the value (3.74 km/s) predicted by equation 5. The lower crustal Vs for unserpentinized rocks, 4.0 km/s, is slightly higher than the value (3.95 km/s) predicted by equation 1. The assumed density, 3000 kg/m^3, lies between values predicted by equations 6 and 8, 2940 kg/m^3 and 3026 kg/m^3, respectively.

Seawater

For the seawater, I assume the following constant values:

(eqn. 53) Vp (km/s) = 1.5, Vs (km/s) = 0, ρ (kg/m^3) = 1000.

Discussion

All the compressional-wave versus depth curves used in USGS Bay Area Velocity Model 05.0.0 are compared in Figure 15A. A similar comparison of the shear-wave velocity versus depth profiles used in the model is presented in Figure 15B. As described earlier, the new empirical Vs versus Vp relations (equations 1 to 5) used in the new velocity model represent its single greatest improvement over its 1997 counterpart (Brocher et al., 1997).

Perhaps the most interesting observations resulting from the comparison of the Vp and Vs versus depth curves in Figure 15 are the differences between the relative ordering of the rock types as a function of Vp versus Vs. These differences result from using different relations to convert Vp to Vs.

An important example of this reversal can be found for greenstones and granites, which are important constituents of the crust in the Bay Area. Whereas the Vp for greenstones is higher than for granites, these two rock types have nearly identical Vs below 5 km. Greenstones can form a significant but variable component of the Franciscan Complex, and have a nearly identical Vs as the Franciscan Complex (Figure 15). Thus, increasing the greenstone content of the Franciscan Complex increases Vp but does not substantially increase Vs.

Another, but more minor, example of this reversal is provided by the contrast between basalts and the Great Valley Sequence (Figure 15). The Vp of Great Valley Sequence is lower than that for basalts at depths above 12 km, but starting at depths of around 7 km, the Vs of the Great Valley Sequence (Older Cenozoic rocks) is comparable or higher than for basalts (Figure 15). This phenomena might lead to the mis-interpretation of Great Valley Sequence as crystalline rocks if only Vs data were available.

For andesites, basalts, gabbros, greenstones, meta basalts, and serpentinites, the curves below 5 km depth in Figure 15 are constrained almost solely by means of laboratory measurements of hand samples (Christensen and Mooney, 1995). The standard deviations of these measurements are generally about 0.25 km/s, but are nearly twice as high for basalts and meta basalts. Fortunately, for granites and the Franciscan Complex, the two most important

constituents of the crust in Northern California, there are many other measurements available for depths greater than 5 km (Figures 4A and 5B). For both the Franciscan Complex and Salinian and Sierran granites, there are a large number of seismic tomography data available which are compatible with the laboratory measurements (Figures 4A and 5B, Table 1).

Equation 16 for Franciscan Complex rocks matches USGS 30-m VSP data, borehole sonic and suspension logs, shallow seismic tomography, and laboratory measurements (Figure 4A). Suspension log data from the QUAD borehole in Santa Clara Valley (Figure 12), are considered especially reliable, and appear to match the VSP velocities near the surface. The shallow tomography data are consistent with a Vp of about 5 km/s at 2 km depth.

Similarly, equations 20 and 21 for granites match sonic log data (Figure 5A), especially data from the SAFOD Pilot Hole and offshore wells OCS #39 and 41 in the Bodega Basin (Figure 6), that are considered very reliable. These equations underpredict USGS 30-m VSP data and some shallow tomography results (Zoback and Wentworth, 1986; Parsons and Zoback, 1997). It would be possible to better fit the USGS 30-m VSP data by increasing the Vp of equation 20 at the surface (to 2.5 km/s) at the expense of not fitting observations of highly fractured granites in the Law CD-#1 sonic log (Figure 4A). It is hoped that model testing will provide insight into this alternate for equation 20.

Figure 15 predicts that the juxtaposition of either granites and gabbros against Franciscan Complex, as along the San Andreas fault, yields a significant Vs contrast but only in the upper 12 km of the crust. For depths greater than 20 km the contrast in Vs between Franciscan Complex and granites decreases to values less than 0.1 km/s. Lateral refraction of seismic energy along the San Andreas fault, consistent with higher Vp and Vs west of the fault as predicted by the relations in Figure 15, is needed to explain observations of strong ground motions produced by the 1989 Loma Prieta earthquake (Stidham et al., 1999).

ACKNOWLEDGEMENTS

This work was supported by the National Earthquake Hazards Reduction Program. Carl Wentworth provided borehole logs in Quaternary deposits from Santa Clara Valley. Naomi Boness provided the SAFOD Pilot Hole Vp and Vs logs. Nick Christensen provided unpublished laboratory Vp measurements of samples from Loma Prieta.

Vicki Langenheim and Bill Stephenson kindly reviewed an earlier version of this report.

REFERENCES CITED

Beaudoin, B. C., N. J. Godfrey, S. L. Klemperer, C. Lendl, A. M. Trehu, T. J. Henstock, A. Levander, J. E. Hole, A. S. Meltzer, J. H. Luetgert, and W. D. Mooney (1996). Transition from slab to slabless: Results from the 1993 Mendocino triple junction seismic experiment, *Geology* **24**, 195-199.

Blakely, R. J., T. M. Brocher, and R. A. Wells (2005). Subduction-zone magnetic anomalies and implications for hydrated upper mantle, *Geology*, 33, 445-448.

Boatwright, J. L. Blair, R, Catchings, M. Goldman, F. Perosi, and C. Steedman (2004). Using twelve years of USGS refraction lines to calibrate the Brocher and others (1997) 3D velocity model of the Bay Area, *U.S. Geol. Surv. Open-File Rept.* **2004-1282**.

Boness, N. L., and M. D. Zoback (2004). Stress-induced seismic velocity and physical properties in the SAFOD Pilot Hole in Parkfield, CA, *Geophys. Res. Lett.* **31**, L15S17, doi: 10.1029/2003GL019020.

Boore, D. M. (2003). A compendium of P- and S-wave velocities for surface-to-borehole logging: Summary and reanalysis of previously published data and analysis of unpublished data, *U.S. Geol. Surv. Open-File Rept.* **03-191**, 14 p. http://geopubs.wr.usgs.gov/open-file/of03-191/.

Borcherdt, R.D., and G. Glassmoyer (1992). Influence of local geology on strong and weak ground motions recorded in the San Francisco Bay region and their implications for site-specific building-code provisions, The Loma Prieta, California, earthquake of October 17, 1989: Strong ground motion and ground failure, *U.S. Geol. Surv. Prof. Paper*, A77-A107.

Brocher, T. M. (2005a). Empirical relations between elastic wavespeeds and density in the Earth's crust, *Bull. Seism. Soc. Am.*, in press.

Brocher, T. M. (2005b). A regional view of urban sedimentary basins in northern California based on oil industry compressional-wave velocity and density logs, *Bull. Seism. Soc. Am.*, in press.

Brocher, T. M., and E. Horta (1998). Compilation of 19 sonic and density logs from 10 oil test wells in the Cape Blanco area, southwestern Oregon, *U.S. Geol. Surv. Open-File Rept.* ***98-237***, 38 p. http://pubs.er.usgs.gov/pubs/ofr/ofr98237

Brocher, T. M., and A. L. Ruebel (1998). Compilation of 29 sonic and density logs from 23 oil test wells in western Washington State, *U.S. Geol. Surv. Open-File Rept.* **98-249**, 41 p. http://pubs.er.usgs.gov/pubs/ofr/ofr98249

Brocher, T. M., and N. I. Christensen (2001). Density and velocity relationships for digital sonic and density logs from coastal Washington and laboratory measurements of Olympic Peninsula mafic rocks and greywackes, *U.S. Geol. Surv. Open-File Rept.* **01-264**, 39 p. http://pubs.er.usgs.gov/pubs/ofr/ofr01264/

Brocher, T.M., J. McCarthy, P.E. Hart, W.S. Holbrook, K.P. Furlong, T.V. McEvilly, J.A. Hole, and S.L. Klemperer (1994). Seismic evidence for a lower-crustal detachment beneath San Francisco Bay, California, *Science* **265**, 1436-1439.

Brocher, T. M., P. E. Hart, W. C. Hunter, and V. E. Langenheim (1996). Hybrid-source seismic reflection profiling across Yucca Mountain, Nevada: Regional lines 2 and 3: *U.S. Geol. Surv. Open-File Rept.* **96-28**, 110 p. http://pubs.er.usgs.gov/pubs/ofr/ofr9628

Brocher, T. M., E. E. Brabb, R. D. Catchings, G. S. Fuis, T. E. Fumal, R. A. Jachens, A. S. Jayko, R. E. Kayen, R. J. McLaughlin, T. Parsons, M. J. Rymer, R. G. Stanley, and C. M. Wentworth (1997). A crustal-scale 3-D seismic velocity model for the San Francisco Bay area, California, *Eos Trans. AGU*, Suppl., 78(46), F435-6.

Brocher, T. M., W. C. Hunter, and V. E. Langenheim (1998). Implications of seismic reflection and potential field geophysical data on the structural framework of the Yucca Mountain-Crater Flat region, Nevada, *Geol. Soc. Am. Bull.* **110**, 947-971.

Brocher, T.M., U.S. ten Brink, and T. Abramovitz (1999). Synthesis of crustal seismic structure and implications for the concept of a slab gap beneath Coastal California, *International Geology Rev.*, v. 41, p. 263-274.

Castagna, J. P., M. L. Batzle, and R. L. Eastwood (1985). Relationships between compressional-wave and shear-wave velocities in clastic silicate rocks, *Geophysics* **50**, 571-581.

Castillo, D.A., and W.L.Ellsworth (1993). Seismotectonics of the San Andreas fault system between Point Arenas and Cape Mendocino in northern California: Implications for the development and evolution of a young transform, *J. Geophys. Res.* **98**, 6543-6560.

Christensen, N. I. (1978). Ophiolites, seismic velocities and oceanic crustal structure, *Tectonophysics* **47**, 131-157.

Christensen, N. I. (1996). Poisson's ratio and crustal seismology, *J. Geophys. Res.* **101**, 3139-3156.

Christensen, N. I., and W. D. Mooney (1995). Seismic velocity structure and composition of the continental crust: A global view, *J. Geophys. Res.* **100**, 9761-9788.

Colburn, R. H., and W. D. Mooney (1986). Two-dimensional velocity structure along the synclinal axis of the Great Valley, California, *Bull. Seism. Soc. Am.* **76**, 1305-1322.

Fletcher, J. B., J. Boatwright, and A. G. Lindh (2003). Wave propagation and site response in the Santa Clara Valley, *Bull. Seism. Soc. Am.* **93**, 480–500.

Fliedner, M. M., S. L. Klemperer, and N. I. Christensen (2000). Three-dimensional seismic model of the Sierra Nevada arc, California, and its implications for crustal and upper mantle composition, *J. Geophys. Res.* **105**, 10899-10921.

Fumal, T. E. (1978). Correlations between seismic wave velocities and physical properties of near-surface geologic materials in the southern San Francisco Bay region, California, *U.S. Geol. Surv. Open-File Rept.* **78-1067**, 114 p.

Gardner, G. H. F., L. W. Gardner, and A. R. Gregory (1984). Formation velocity and density - The diagnostic basics for stratigraphic traps, *Geophysics* **39**, 770-780.

Gibbs, J. F., D. M. Boore, W. B. Joyner, and T. E. Fumal (1994). The attenuation of seismic shear waves in Quaternary alluvium in Santa Clara Valley, California: *Bull. Seism. Soc. Am.* **84**, 76-90.

Godfrey, N. J., B. C. Beaudoin, S. L. Klemperer, and the Mendocino Working Group USA (1997). Ophiolitic basement to the Great Valley forearc basin, California, from seismic and gravity data: Implications for crustal growth at the North American continental margin, *Geol. Soc. Am. Bull.* **109**, 1536-1562.

Griscom, A., and R. C. Jachens (1990). Tectonic implications of gravity and magnetic models along east-west profiles across the Great Valley near Coalinga, Chap. 5 of M.J. Rymer and W.L. Ellsworth, eds., The Coalinga, California, earthquake of May 2, 1983: *U.S. Geol. Surv. Prof. Paper* **1487**, p. 69-78.

Hamilton, E. L. (1972). Compressional-wave attenuation in marine sediments, *Geophysics* **37**, 620-646.

Hardebeck, J. L., A. J. Michael, and T. M. Brocher (2004). Seismic velocity structure and seismotectonics of the Hayward fault system, east San Francisco Bay, California, *Eos Trans. AGU*, 85(47), Fall Mtg. Suppl., Abstract S34A-05.

Hauksson, E., D. Oppenheimer, and T. M. Brocher (2004). Imaging the source region of the 2003 San Simeon earthquake within the weak Franciscan subduction complex, central California, *Geophys. Res. Lett.* **31**, L20607, doi:10.1029/2004GL021049.

Hoffman, L. R., and W. D. Mooney (1984). A seismic study of Yucca Mountain and vicinity, southern Nevada; Data report and preliminary results: *U.S. Geol. Surv. Open-File Rept.* **83-588**, 50 p.

Holbrook, W. S. and W. D. Mooney (1987). The crustal structure of the axis of the Great Valley, California, from seismic refraction measurements, *Tectonophysics* **140**, 49-63.

Holbrook, W.S., T.M. Brocher, U.S. ten Brink, and J.A. Hole (1996). Crustal structure beneath the San Francisco Bay block and the central California continental margin, *J. Geophys. Res.* **101**, 22,311-22,334.

Hole, J. A., T. M. Brocher, S. L. Klemperer, T. Parsons, H. M. Benz, and K. P. Furlong (2000). Three-dimensional seismic velocity structure of the San Francisco Bay area, *J. Geophy. Res.*, **105**, 13,859-13,874.

Jachens, R. C., and A. Griscom (2004). Geophysical and geological setting of the earthquake, inferred from gravity and magnetic anomalies, in the Loma Prieta, California, earthquake of October 17, 1989—Geologic setting and crustal structure, R.E. Wells, ed., *U. S. Geol. Surv. Prof. Pap. 1550-E, E49-E80.*

Johnston, D. H. (1981). Attenuation: A state of-the-art summary, in Seismic Wave Attenuation, ed. by D.H. Johnston and M.N. Toksoz*, Society of Exploration Geophysicists, Geophysics reprint series* **2**, 123-139.

Joyner, W. B. (2000). Strong motion from surface waves in deep sedimentary basins, *Bull. Seism. Soc. Am.* **90**, S95-S112.

Kudo, K. and E. Shima (1970). Attenuation of shear waves in soil, *Bull. Earthquake Res. Inst.* **48**, 145-158.

Langenheim, V. E., K. M. Schmidt, and R. C. Jachens (1997). Coseismic deformation during the 1989 Loma Prieta earthquake and range-front thrusting along the southwestern margin of the Santa Clara valley, California, *Geology* **25**, 1091-1094.

Levander, A.R. and R.L. Kovach (1990). Shear velocity structure of the northern California lithosphere, *J. Geophys. Res.* **95**, 19,773-19,784.

Liu, H. P., R. E. Warrick, R. E. Westerlund, and R. E. Kayen (1994). In situ measurement of seismic shear-wave absorption in the San Francisco Holocene bay mud by the pulse-broadening method, *Bull. Seism. Soc. Am.* **84**, 62-75.

Ludwig, W. J., J. E. Nafe, and C. L. Drake (1970). Seismic refraction, in *The Sea,* A. E. Maxwell, (Editor) Vol. 4, Wiley-Interscience, New York, 53–84.

MacGregor-Scott, N., and A. Walter (1988). Crustal velocities near Coalinga, California, modeled from a combined earthquake/explosion refraction profile, *Bull. Seism. Soc. Am.* **78**, 1475-1490.

Majer, E., T. V. McEvilly, F. S. Eastwood, and L. R. Meyer (1988). Fracture detection using P- and S-wave vertical seismic profiling at The Geysers, *Geophysics* **53**, 76-84.

Martin, R. J., III, R. H. Price, P. J. Boyd, and J. S. Noel (1994). Bulk and mechanical properties of the Paintbrush Tuff recovered from Borehole USWS NRG-6: Data report, Sandia Report, SAND93-4020, UC-814, 92 p.

Martin, R. J., III, R. H. Price, P. J. Boyd, and J. S. Noel (1995). Bulk and mechanical properties of the Paintbrush Tuff recovered from Borehole USWS NRG-7/7A: Data report, Sandia Report, SAND94-1996, UC-814, 93 p.

Mavko, G., T. Mukerji, and J. Dvorkin (1998). *The Rock Physics Handbook: Tools for Seismic Analysis in Porous Media*, 329 pp. (Cambridge University Press, U.K.).

McCulloch, D. S. (1987). Regional geology and hydrocarbon potential of offshore Central California, in Geology and Resource Potential of the Continental Margin of Western North America and adjacent ocean basins-Beaufort Sea to Baja California, D.W. Scholl, A. Grantz, and J.G. Vedder, eds., Circum-Pacific Council for Energy and Mineral Resources, Earth Science Series, Vol. 6, p. 353-401.

Meltzer, A. S., A. R. Levander, and W. D. Mooney (1987). Upper crustal structure, Livermore Valley and vicinity, California coast ranges, *Bull. Seism. Soc. Am.* **77**, 1655-1673.

Mooney, W. D., and S. Schapper (1995). Seismic refraction studies (Chapter 5) *in* Oliver, H.W., Ponce, D.A., and Hunter, W. Clay, eds., Major results of geophysical investigations at Yucca Mountain and vicinity, southern Nevada: *.S. Geol. Surv. Open-file Rept* **95-74**, p. 99-119.

Newhouse, M. W., R. T. Hanson, C.M. Wentworth, R. R. Everett, C. F. Williams, J. C. Tinsley, T. E. Noce, and B. A. Carkin (2004). Geologic, water-chemistry, and hydrologic data from multiple-well monitoring sites and selected water-supply wells in the Santa Clara Valley, California, 1999–2003, *U.S. Geol. Surv. Scient. Invest. Rep. 2004-5250,* 142 p.

Olsen, K. B., S. M. Day, and C. R. Bradley (2003). Estimation of *Q* for long-period (2 sec) waves in the Los Angeles Basin, *Bull. Seism. Soc. Am.* **93**, 627–638.

Oppenheimer, D.H. and J.P. Eaton (1984). Moho orientation beneath central California from regional earthquake travel times, *J. Geophys. Res.* **89**, 10267-10282.

Parsons, T., and M. L. Zoback (1997). Three dimensional upper crustal velocity structure beneath San Francisco Peninsula, California, *J. Geophys. Res.* **102**, 5473-5490.

Parsons, T., R. J. Blakely, and T. M. Brocher (2001). A simple algorithm for sequentially incorporating gravity observations in seismic traveltime tomography, *International Geology Review, 43*, 1073-1086.

Ponce, D.A., T. G. Hildenbrand, and R. C. Jachens (2003). Gravity and magnetic expression of the San Leandro gabbro with implications for the geometry and evolution of the Hayward fault zone, northern California, *Bull. Seism. Soc. Am.* **93**, 14-26.

Price, R. H., R. J. Martin, III, and R. W. Haupt (1994). The effect of frequency on Young's modulus and seismic wave attenuation, Sandia Report, SAND92-0847, UC-814, 50 p.

Saad, A. F. (1969). Magnetic properties of ultramafic rocks from Red Mountain, California, *Geophysics* **34**, 974-987.

Smith, N. (1992). Gravity interpretation of San Pablo Bay and vicinity: in Field Trip Guide to Late Cenozoic Geology in the North Bay Region, Wright, T.L., edit., Northern California Geological Society, p. 71-80.

Spieth, M. A., D. P. Hill, and R. J. Geller (1981). Crustal structure in the northwestern foothills of the Sierra Nevada from seismic refraction experiments, *Bull. Seism. Soc. Am.* **71**, 1075-1087.

Stewart, R.M., and L. Peselnick (1978). Systematic behavior of compressional velocity in Franciscan rocks at high pressure and temperature, *J. Geophys. Res.* **83**, 831-839.

Stidham, C., M. Antolik, D. Dreger, S. Larsen, and B. Romanowicz (1999). Three-dimensional structure influences on the strong motion wavefield of the 1989 Loma Prieta earthquake, *Bull. Seism. Soc. Am.* **89**, 1184-1202.

Stierman, D. J., and R. L. Kovach (1979). An in situ velocity study: The Stone Canyon well: *J. Geophys. Res.* **84**, 672-678.

Thompson, G.A., and M. Talwani (1964). Crustal structure from Pacific Basin to central Nevada, J. Geophys. Res., 69, 4813-4837.

Tullos, F. N., and A. C. Reid (1969). Seismic attenuation of gulf coast sediments, *Geophysics* **34**, 516-528.

Walter, A. W., and W. D. Mooney (1982). Crustal structure of the Diablo and Gabilan ranges, central California: A reinterpretation of existing data, *Bull. Seism. Soc. Am.* **72**, 1567-1590.

Wentworth, C. M., M. C. Blake, D. L. Jones, A. W. Walter, and M. D. Zoback (1984). Tectonic wedging associated with emplacement of the Franciscan assemblage, California coast ranges, in Blake, M.C., Jr., ed., Franciscan geology of northern California: Society of Economic Paleotologists and Mineralogists, Pacific Section, vol. 43, p. 163-166.

Wright, T. L., and N. Smith (1992). Right step from the Hayward fault to the Rodgers Creek fault beneath San Pablo Bay, in Borchardt, G., and others, eds., Proceedings of the Second Conference on Earthquake Hazards in the Eastern San Francisco Bay Area: California Department of Conservation, Division of Mines and Geology Special Publication 113, p. 407-417.

Zoback, M. D., and C. M. Wentworth (1986). Crustal studies in central California using an 800-channel seismic reflection recording system, in Reflection Seismology: A global perspective, AGU Geodynamic Series Vol. 13, p. 183-196.

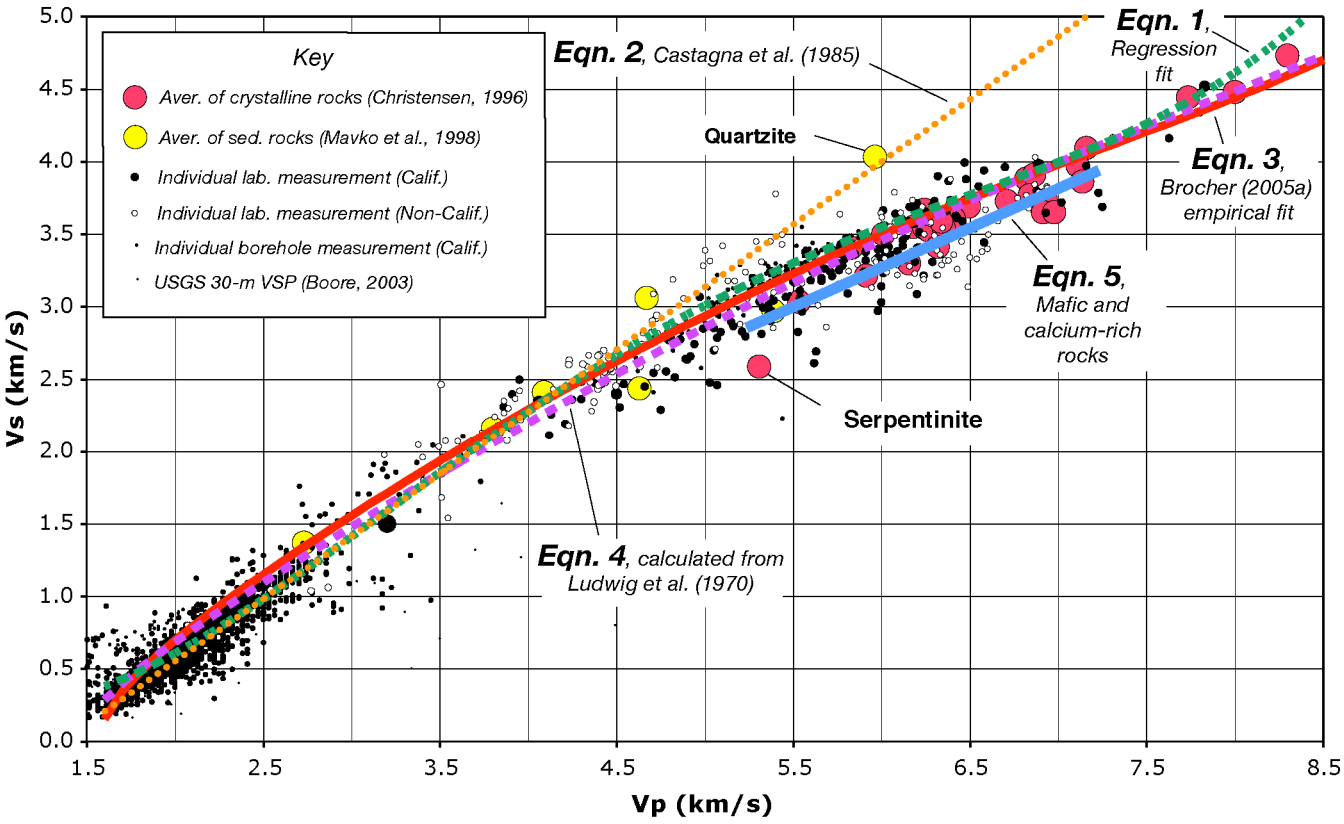

Figure 1. Vs versus Vp for common rock types, modified from Brocher (2005a). Solid circles represent samples from northern and central California; unfilled circles represent other samples. Circle sizes increase qualitatively with data quality (see key): largest circles represent averages of large numbers of individual laboratory measurements, intermediate circles show individual laboratory measurements, smaller circles correspond to individual borehole measurements, and smallest circles correspond to USGS 30-m VSP data. Various regressions to the data are discussed in the text.

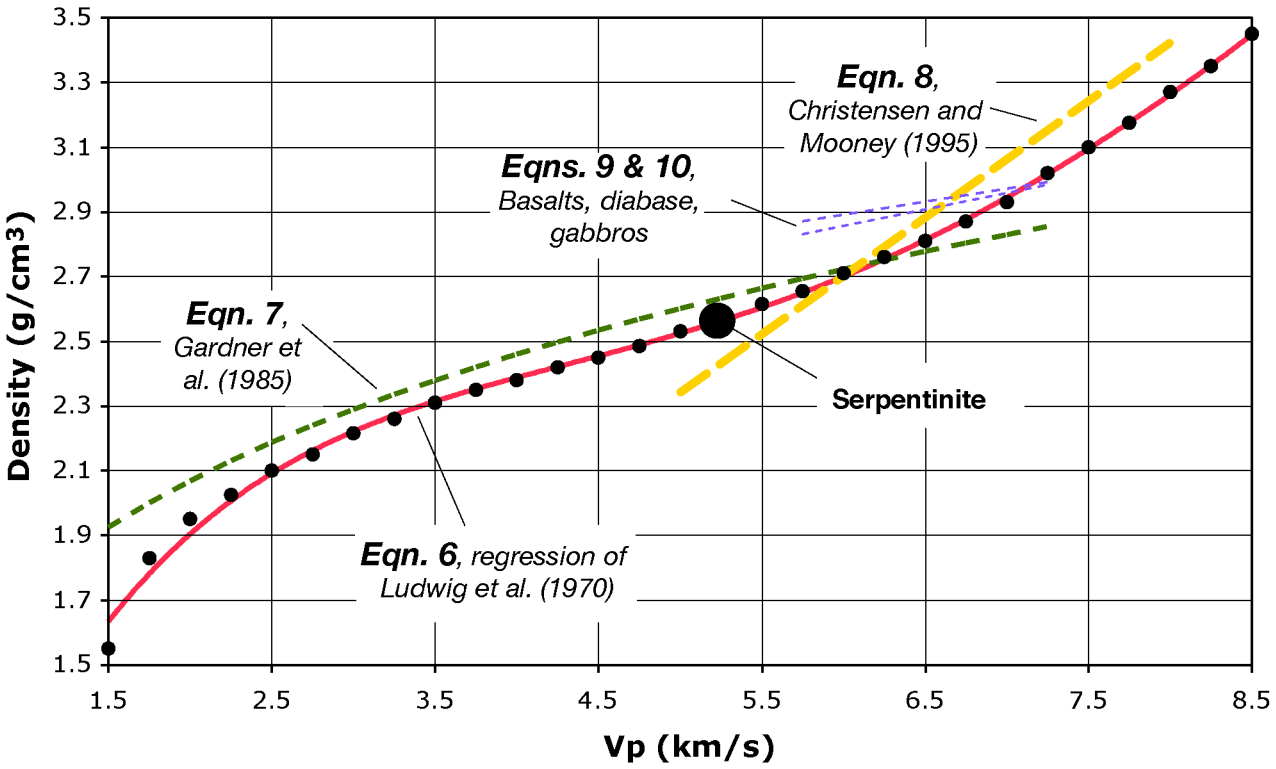

Figure 2. Comparison of density versus Vp relations: equation 6 is the Nafe-Drake curve. Filled circles show handpicks from the Nafe-Drake curve published by Ludwig et al. (1970). Solid line (eqn. 6) shows polynomial fit to these picks. Other lines show relations discussed in the text.

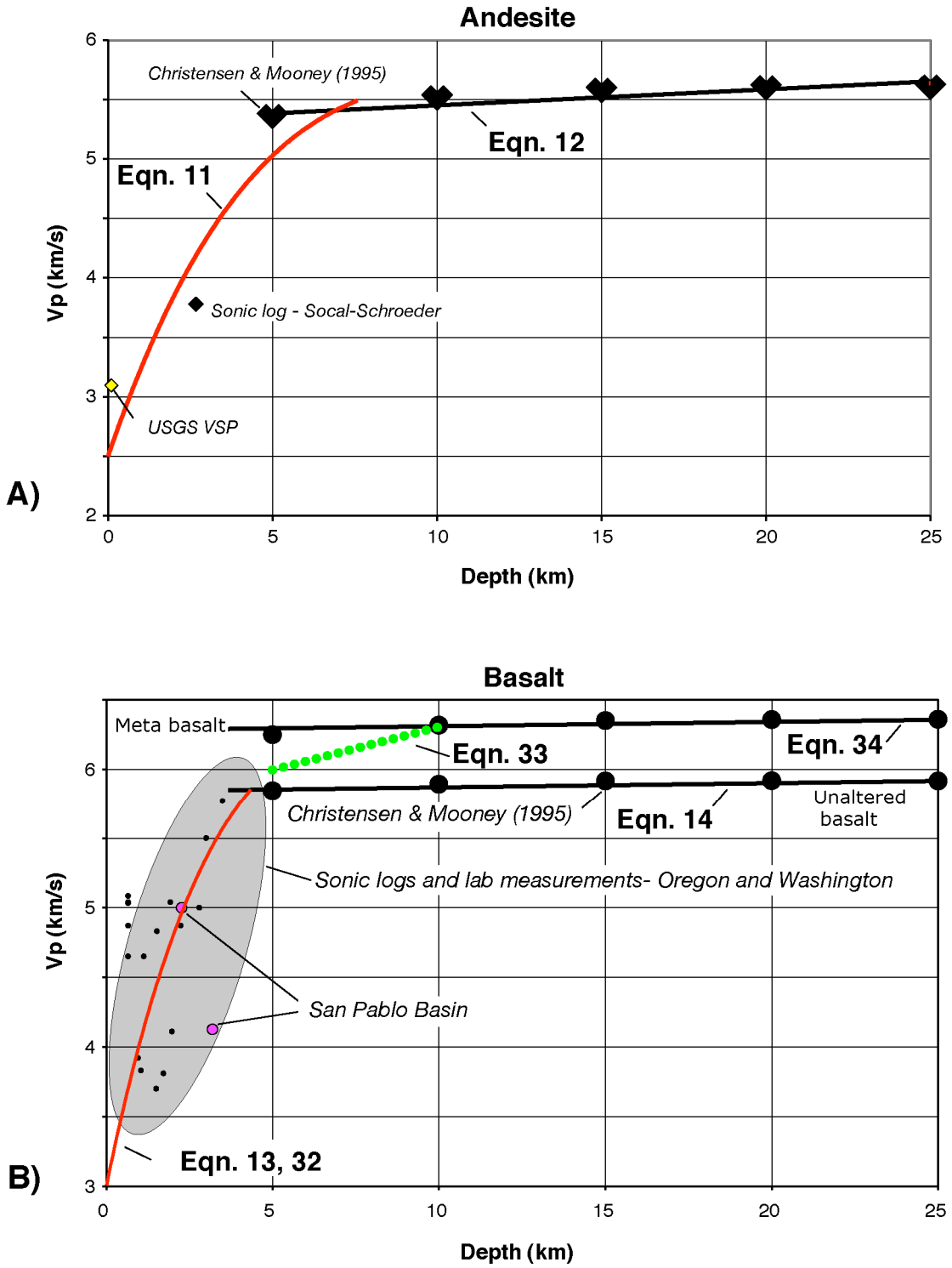

Figure 3. (A) Vp versus depth measurements for andesite. Largest symbols represent means of 30 laboratory measurements on andesites having a standard deviation of 0.2 km/s (Christensen and Mooney, 1995), other data sources are identified in Table 1. Red curve shows non-linear regression of data (equation 11). Solid black line shows equation 12. (B) Vp versus depth measurements for unaltered and meta basalt. Largest symbols show means of 415 and 102 laboratory measurements for unaltered and meta basalts, respectively (Christensen and Mooney, 1995). Red curve shows non-linear regression of data used in equations 13 and 32. Dotted green line shows equation 33. Solid black lines shows equations 14 and 34. Ellipse shaded gray outlines sonic log and laboratory data for basalts from Oregon and Washington (Brocher et al., 1998; Brocher and Horta, 1998; Brocher and Christensen, 2001). Two measurements from San Pablo Basin lying within this ellipse are indicated as pink filled circles (Smith, 1992; Wright and Smith, 1992, Brocher, 2005b).

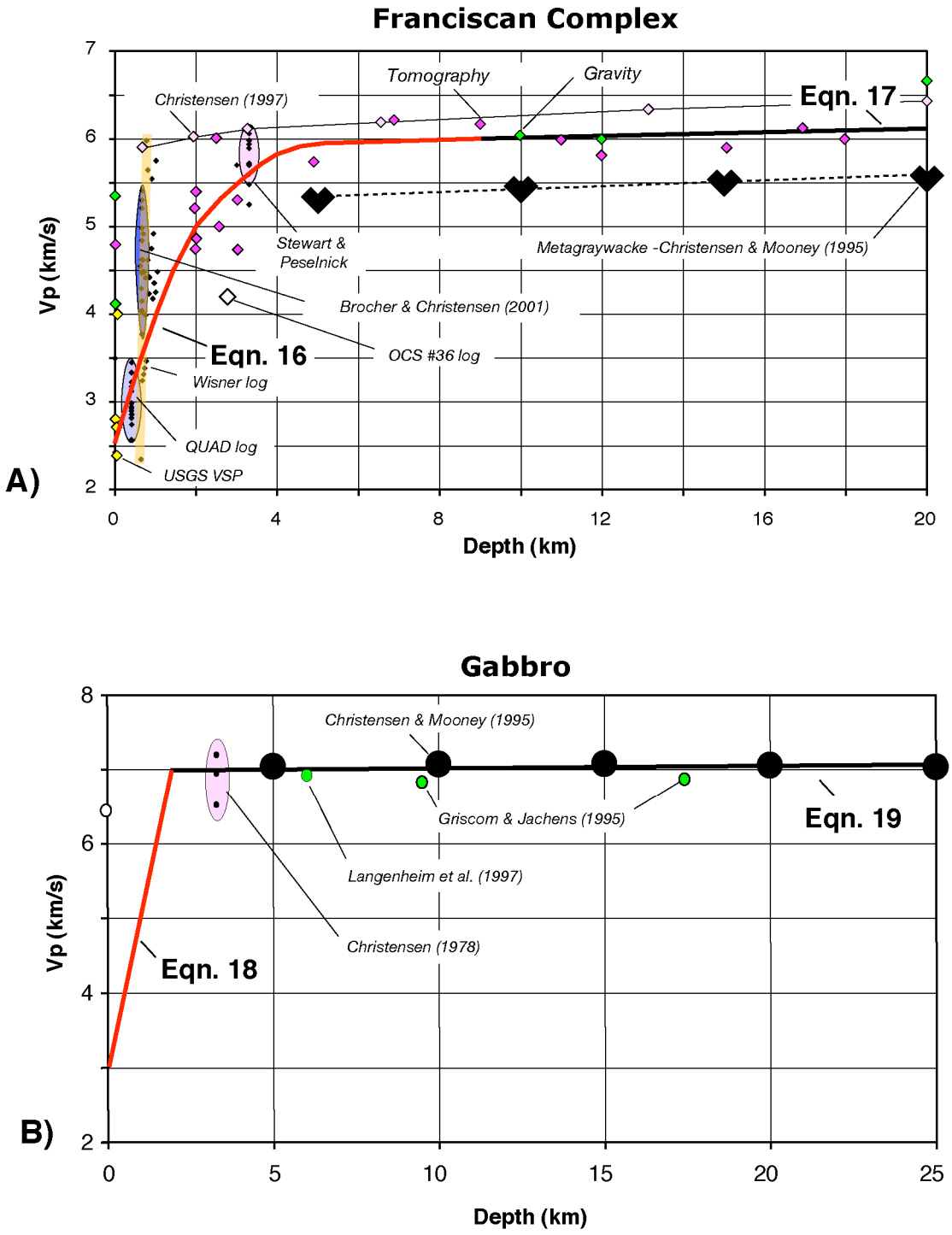

Figure 4. (A) Vp versus depth measurements for Franciscan Complex (or metagraywacke). Large symbols represent means of 87 laboratory measurements of metagraywackes with standard deviations between 0.4 to 0.6 km/s (Christensen and Mooney, 1995). Colored ellipses show clusters of measurements reported by various authors (see Table 1 for details). Unpublished laboratory data for a sample of the Loma Prieta metagraywacke (N. I. Christensen, writ. comm., 1997) have not been corrected for the expected thermal gradient. Purple filled symbols show seismic tomography measurements. Green filled symbols are derived from density models. Pink filled symbols show laboratory measurements of Vp. Red curve shows equation 16: heavy black line shows equation 17. (B) Vp versus depth measurements for gabbro. Large symbols represent means of 187 laboratory measurements of gabbros with a standard deviation of 0.25 km/s (Christensen and Mooney, 1995). Red line shows equation 18: heavy black line shows equation 19.

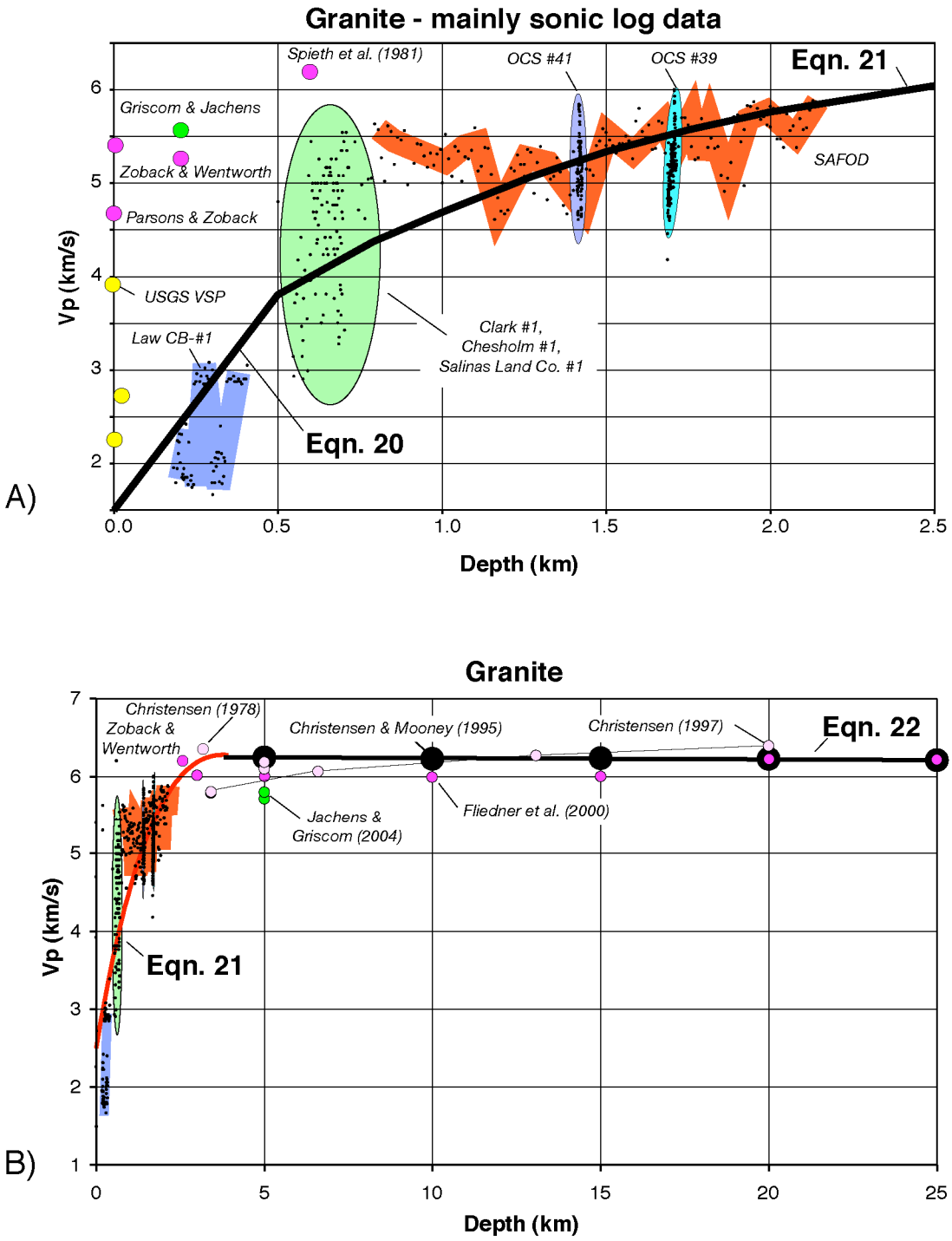

Figure 5. (A) Vp versus depth measurements for granite, showing mainly USGS 30-m VSP, shallow seismic tomography (purple filled symbols), and well log observations to a depth of 2.5 km. Data from individual boreholes (Boness and Zoback, 2004; Brocher, 2005b) are highlighted by thick colored lines or colored ellipses. Table 1 provides additional information on data sources. (B) All Vp versus depth measurements for granite with emphasis on data sources for depths greater than 2.5 km (see Table 1). Largest symbols show means of 134 laboratory measurements of granites with standard deviations of 0.125 km/s (Christensen and Mooney, 1995). Unpublished laboratory data for a granite sampled near Loma Prieta (N. I. Christensen, writ. comm., 1997) have not been corrected for the expected thermal gradient. Red curve shows regression of data used for equation 21.

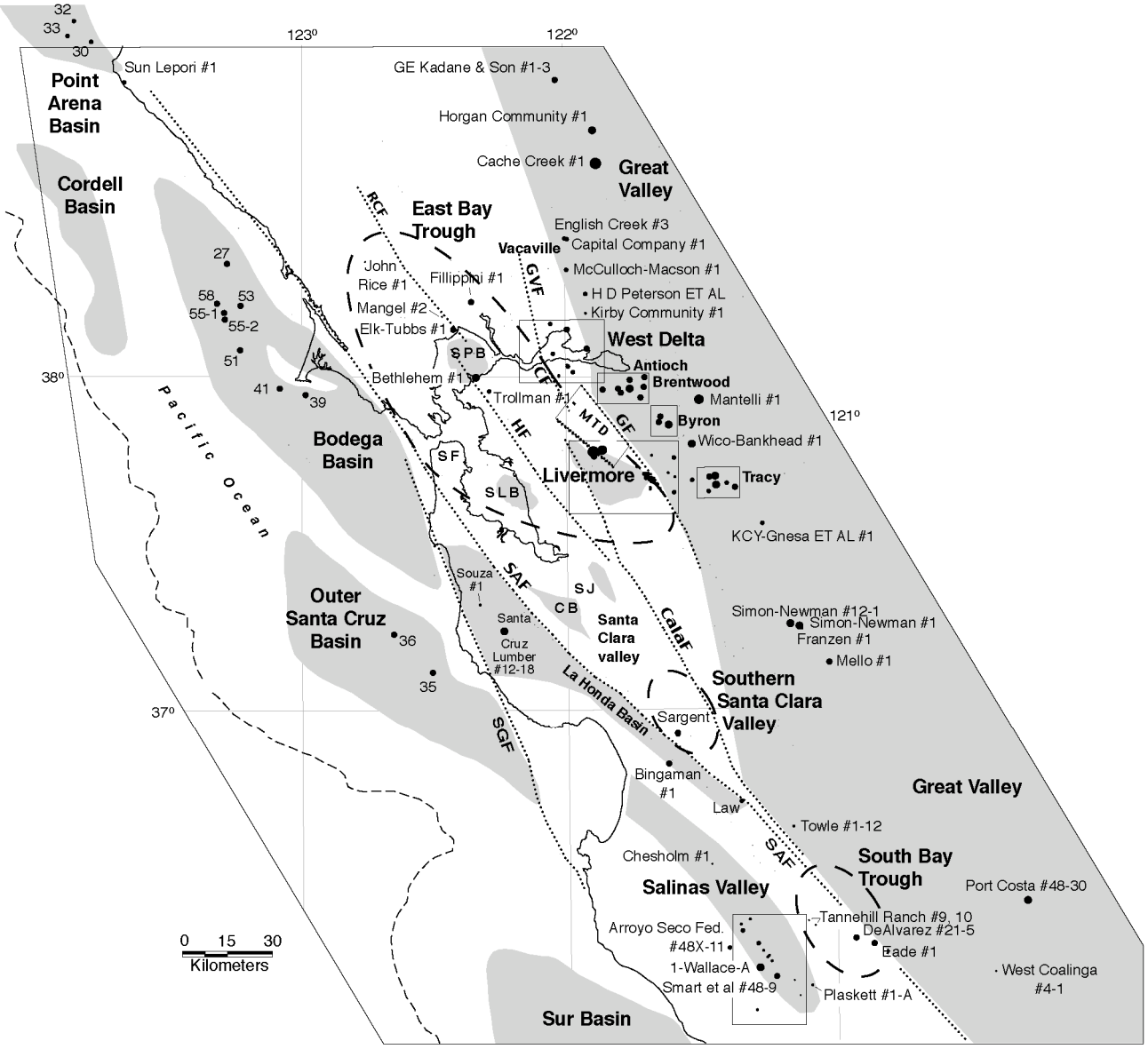

Figure 6. Map showing locations of sedimentary basins (shaded areas) in the greater San Francisco Bay Area, selected crustal faults (dotted lines), and oil industry boreholes (filled circles) studied by Brocher (2005). Size of filled circles for the wells provides a relative estimate of the depth of the borehole. Dashed lines outline the East Bay Trough, the southern Santa Clara Valley, and the South Bay Trough. Abbreviations: CalaF – Calaveras Fault, CB – Cupertino Basin, CF – Concord Fault, GF – Greenville Fault, GVF – Green Valley Fault, HF – Hayward Fault, LHB – La Honda Basin, MTD – Mount Diablo, SAF – San Andreas Fault, SF – San Francisco, SGF- San Gregorio Fault, SJ – San Jose, SLB – San Leandro Basin, and SPB – San Pedro Basin. Rectangles outline clusters of boreholes in the vicinity of the West Delta, Brentwood, Byron, Livermore, Tracy, and Salinas Valley. Offshore basins and borehole locations from McCulloch (1987).

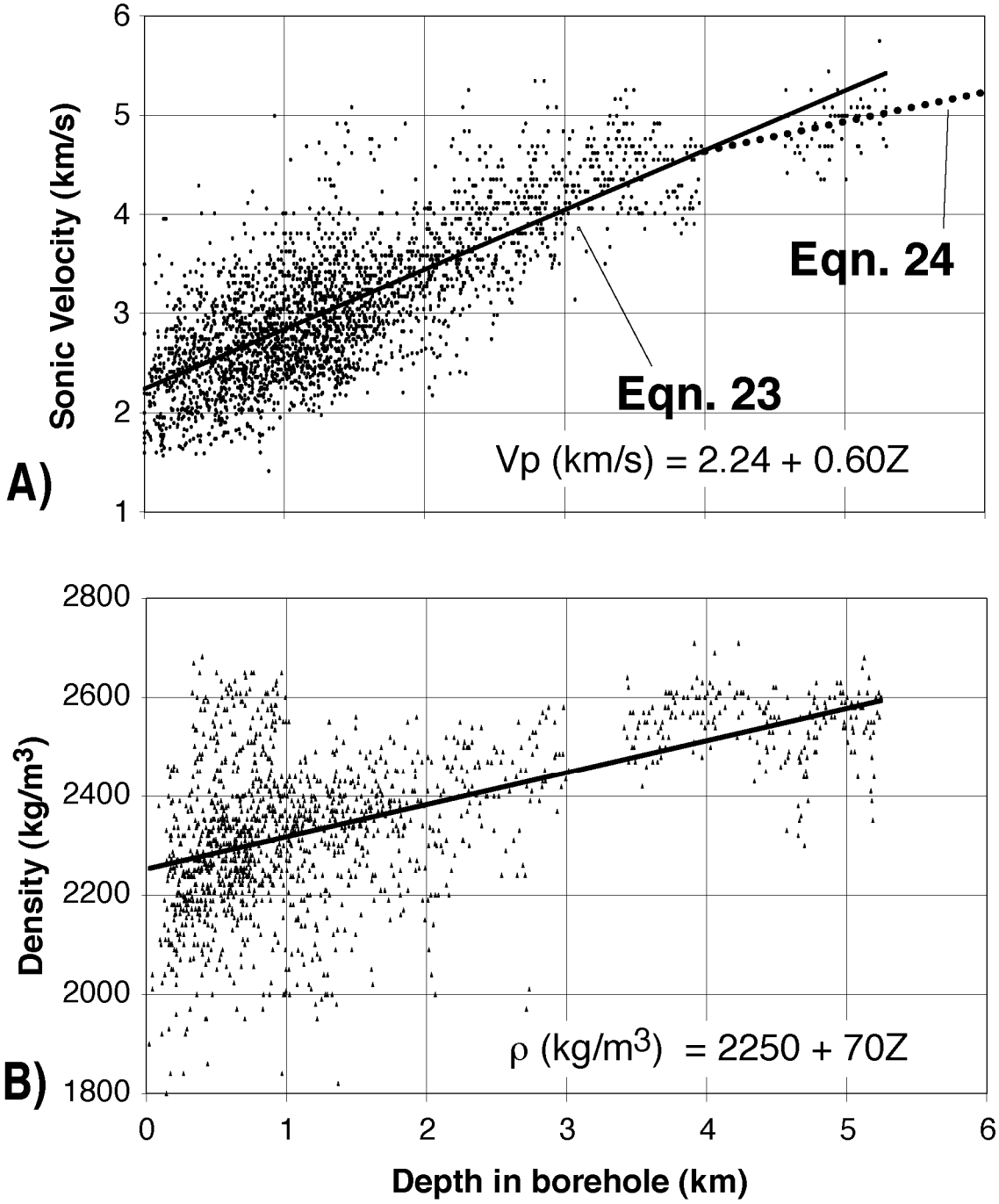

Figure 7. Linear regression of sonic velocity and density logs from 50 boreholes including 17 in the Great Valley, 9 in the West Delta, 15 in the Livermore Valley, and 9 in the East Bay Trough (from Brocher, 2005b). Equation 23 represents the linear regression of these sonic log data.

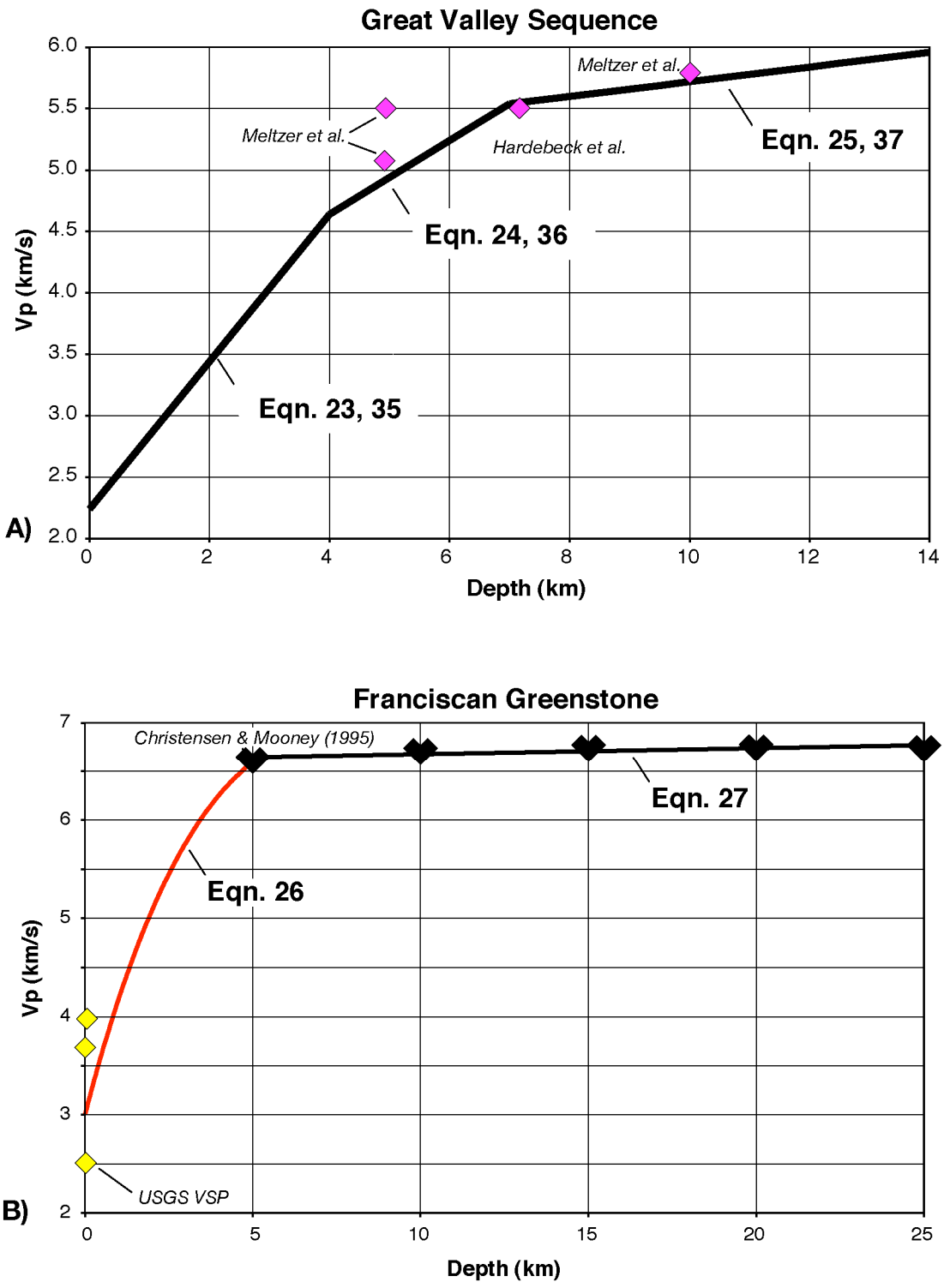

Figure 8. (A) Equations 23 to 25 used to represent Vp versus depth for the Great Valley Sequence, showing seismic refraction/tomography velocities reported by Meltzer et al. (1987) and Hardebeck et al. (2004). (B) Vp versus depth measurements for Franciscan Greenstone (greenschist facies basalt). Largest symbols show means of 63 laboratory measurements of greenschist facies basalt having standard deviations of 0.25 km/s (Christensen and Mooney, 1995). Means of USGS 30-m VSP data are also shown (yellow filled symbols).

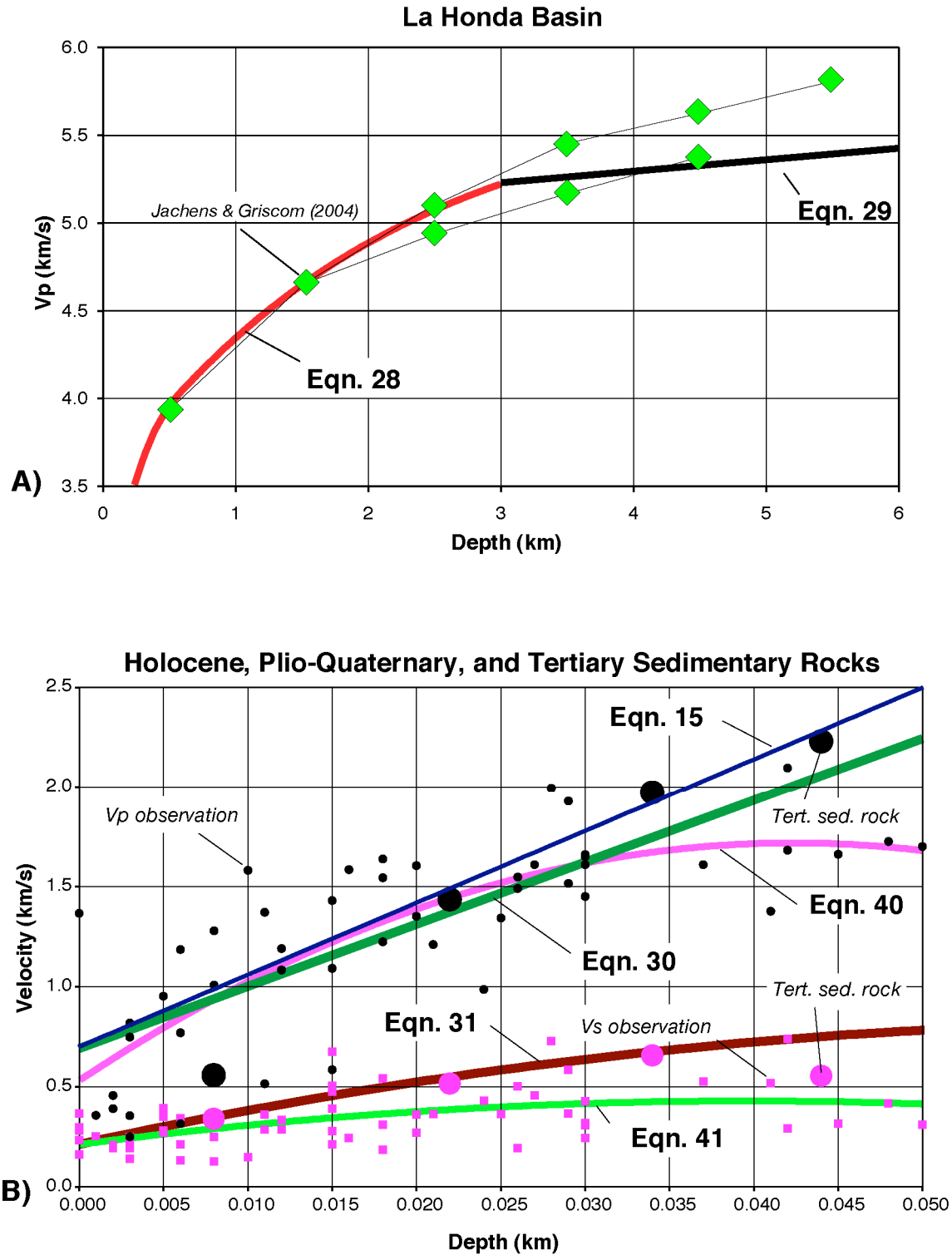

Figure 9. (A) Vp versus depth measurements for Cenozoic sedimentary rocks in the La Honda basin. Measurements are from density models for the basin (Jachens and Griscom, 2004) converted to Vp using equation 6. Equation 28 (red curve) shows regression of the measurements. (B) Vp for depths up to 50 m for Holocene and Plio-Quaternary deposits (small symbols, mainly from Tables 3 and 4) as well as for USGS 30-m VSP measurements for Tertiary sedimentary rocks (large symbols, T. M. Brocher, unpublished compilation, 2005). Equation 15 shows assumed relation for Franciscan Complex metagraywackes at shallow depth. Equations 30 and 31 represent fits to VSP data for Tertiary sedimentary rocks. Equations 40 and 41 represent regression fits to data for Holocene and Plio-Quaternary deposits.

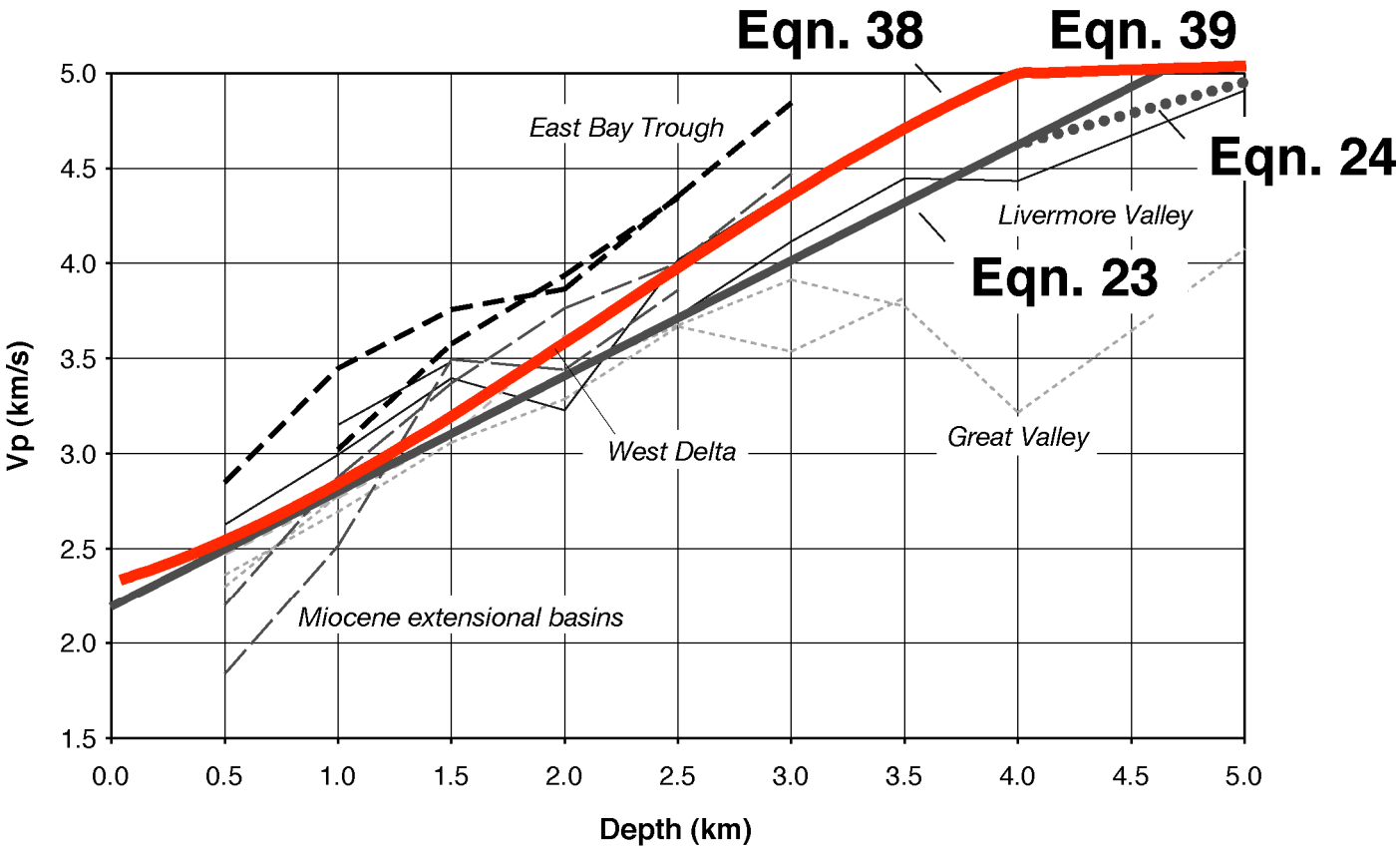

Figure 10. Average velocities within sedimentary basins in the greater San Francisco Bay Area, calculated by averaging the velocities predicted by linear regression of the sonic well logs at 0.5 km intervals (Brocher, 2005b). Averages calculated from the regressions of the upper and lower parts of the logs are shown with identical pattern to emphasize that they yield similar results. Heavy solid line shows the linear regression made directly to a subset of these well log data (described in Figure 7).

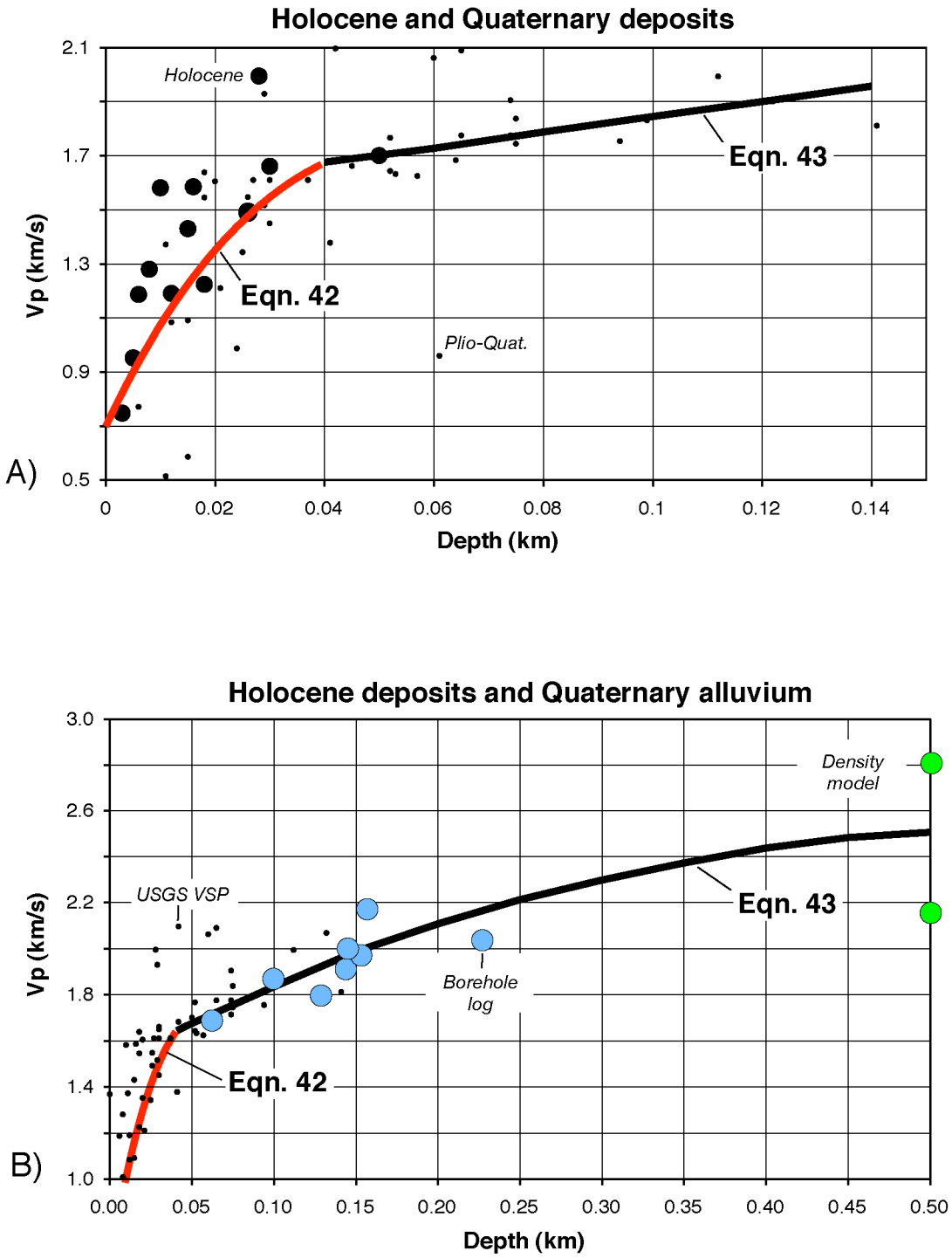

Figure 11. (A) Vp versus depth measurements for Holocene and Plio-Quaternary deposits from means of USGS VSP data to a depth of 150 m from Tables 3 and 4. Largest filled circles represent measurements in Holocene units. (B) All Vp versus depth measurements for Holocene deposits and Plio-Quaternary alluvium compiled from data sources in Table 3 and 4, as well as means of borehole logs from the Santa Clara Valley (filled blue circles: Newhouse et al., 2004; C. M. Wentworth, writ. comm., 2004), and density models (Ponce et al., 2003; Jachens and Griscom, 2004).

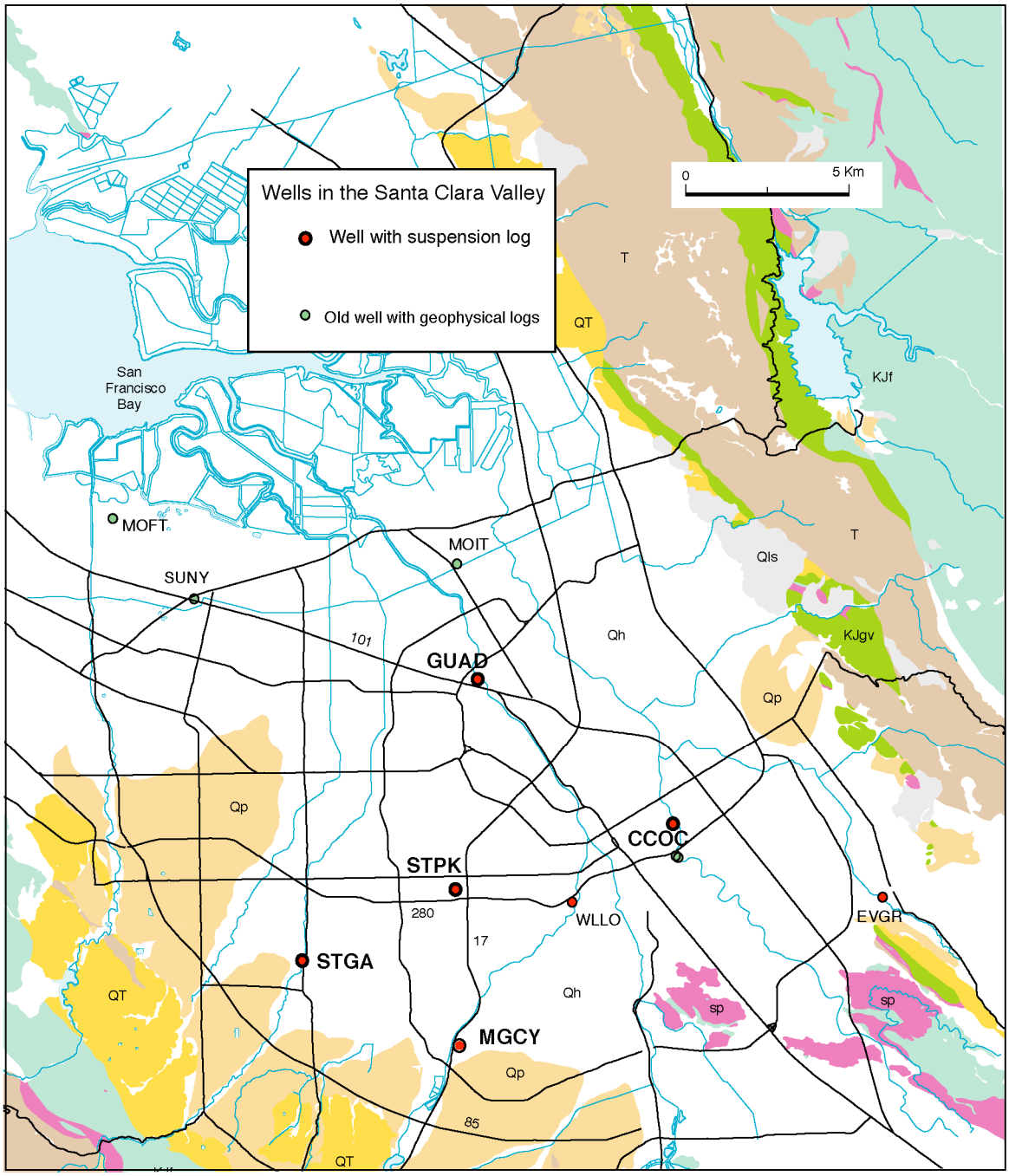

Figure 12. Geologic map showing locations of 300-m to 400-m deep boreholes in Santa Clara Valley, south of San Francisco Bay, for which both Vp and Vs suspension logs were run within the Quaternary alluvium. Modified from Newhouse et al. (2004). Abbreviations: Qh-Holocene age deposits, Qls-Holocene and Pleistocene landslide deposits, Qp-Late-Pleistocene-age deposits, QT-Pliocene-Quaternary age sedimentary deposits (Santa Clara Formation and equivalents), KJf-Franciscan Assemblage, KJgv-Great Valley Sequence, sp-serpentinite and associated Coast Range ophiolite, T-Tertiary-age sedimentary deposits (includes some volcanics and the Monterey Formation).

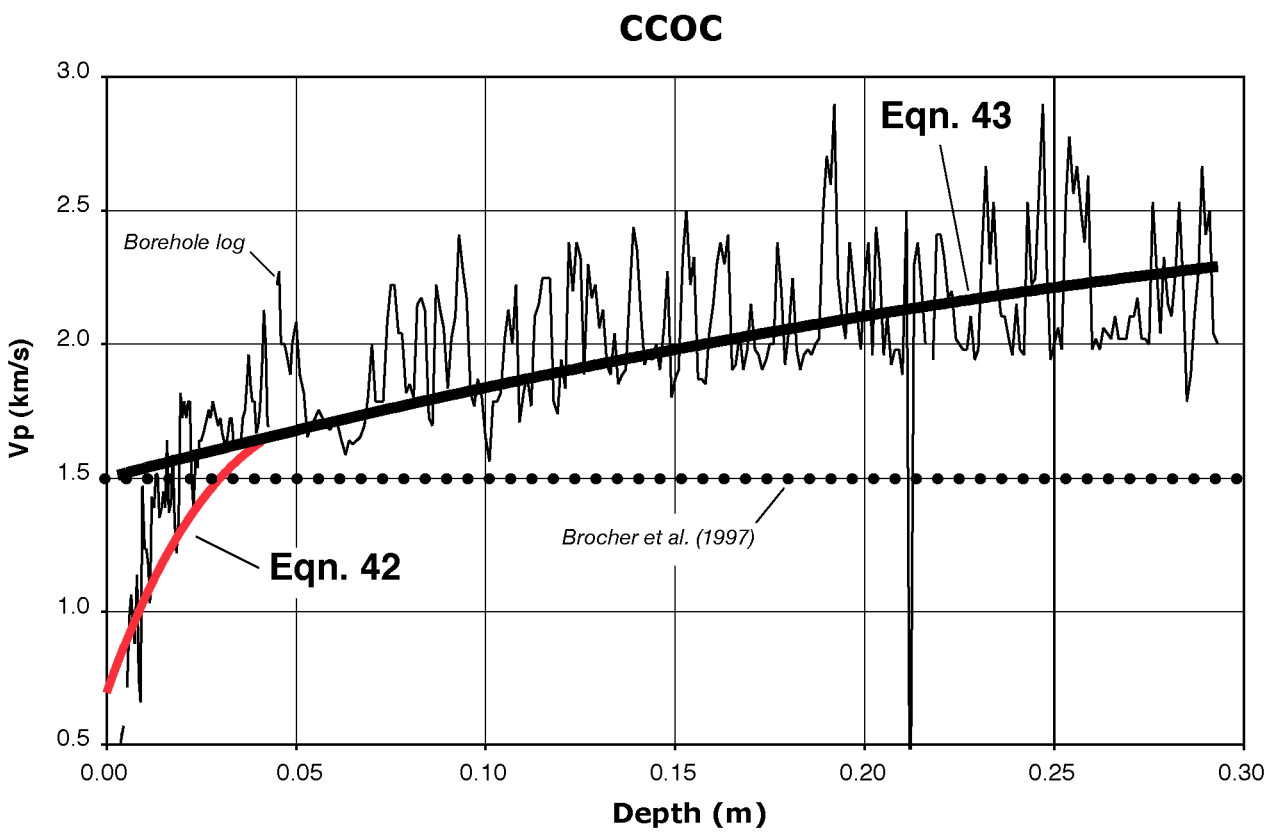

Figure 13. Comparison of equations 42 and 43 for Holocene and Plio-Quaternary deposits with the compressional-wave borehole suspension log for the CCOC borehole in Santa Clara Valley. See Figure 12 for the location of this borehole. Dotted line shows relation used by Brocher et al. (1997) for Holocene and Plio-Quaternary deposits.

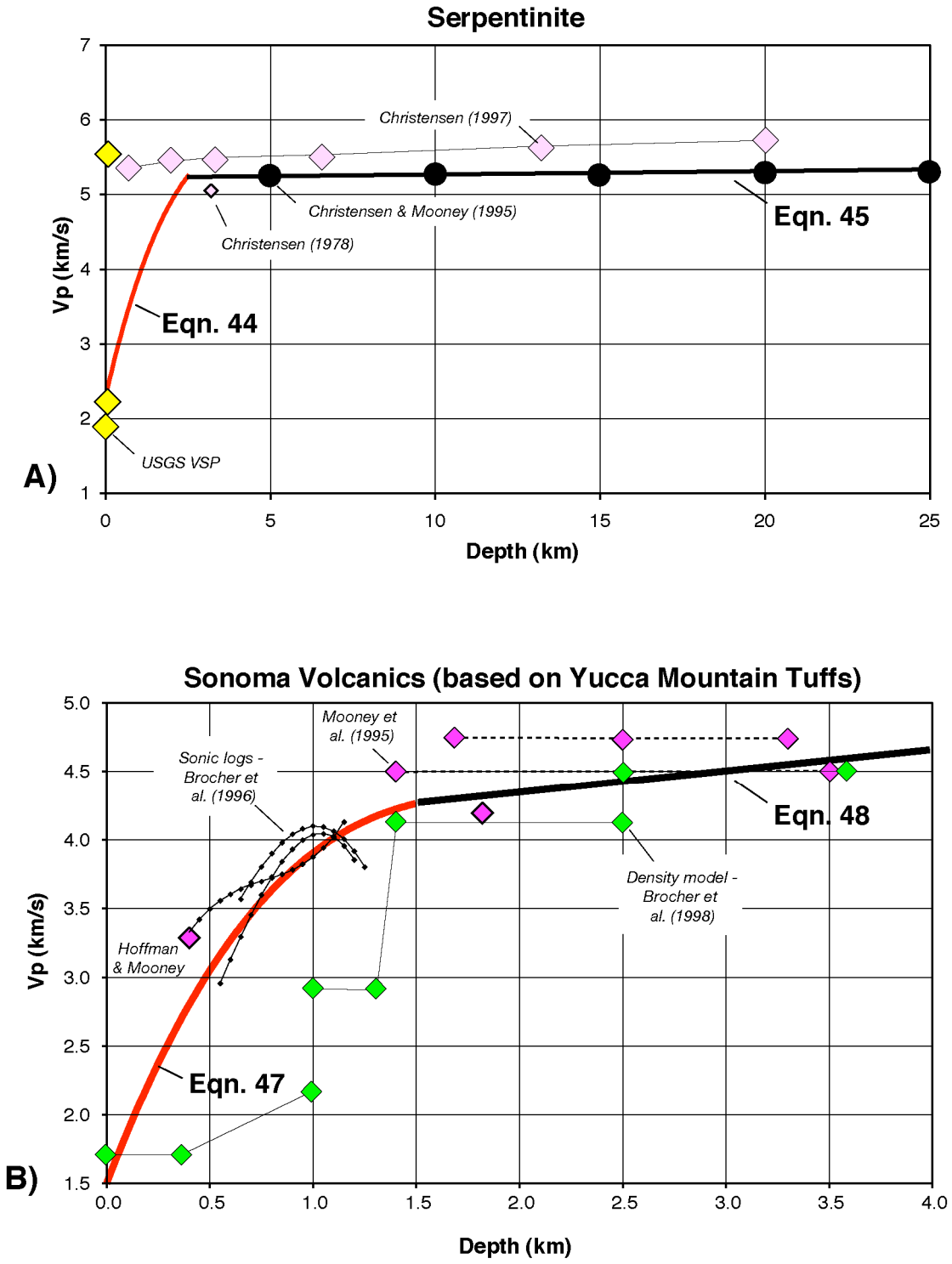

Figure 14. (A) Vp versus depth measurements for serpentinite. Largest symbols show means of 36 laboratory measurements of serpentinite having standard deviations of 0.3 km/s (Christensen and Mooney, 1995). Means of USGS 30-m VSP data are also shown (yellow filled symbols). Unpublished laboratory data for a serpentinite sampled near Loma Prieta (N. I. Christensen, writ. comm., 1997) have not been corrected for the expected thermal gradient. (B) Vp versus depth measurements for Miocene welded and nonwelded tuffs from the vicinity of Yucca Mountain, Nevada, used as a proxy for the Sonoma Volcanics. Data points between 0.5 and 1.25 km depth represent regression of borehole data (Brocher et al., 1996, see Table 1). Seismic refraction measurements by Mooney et al. (1995) are shown as purple filled symbols.

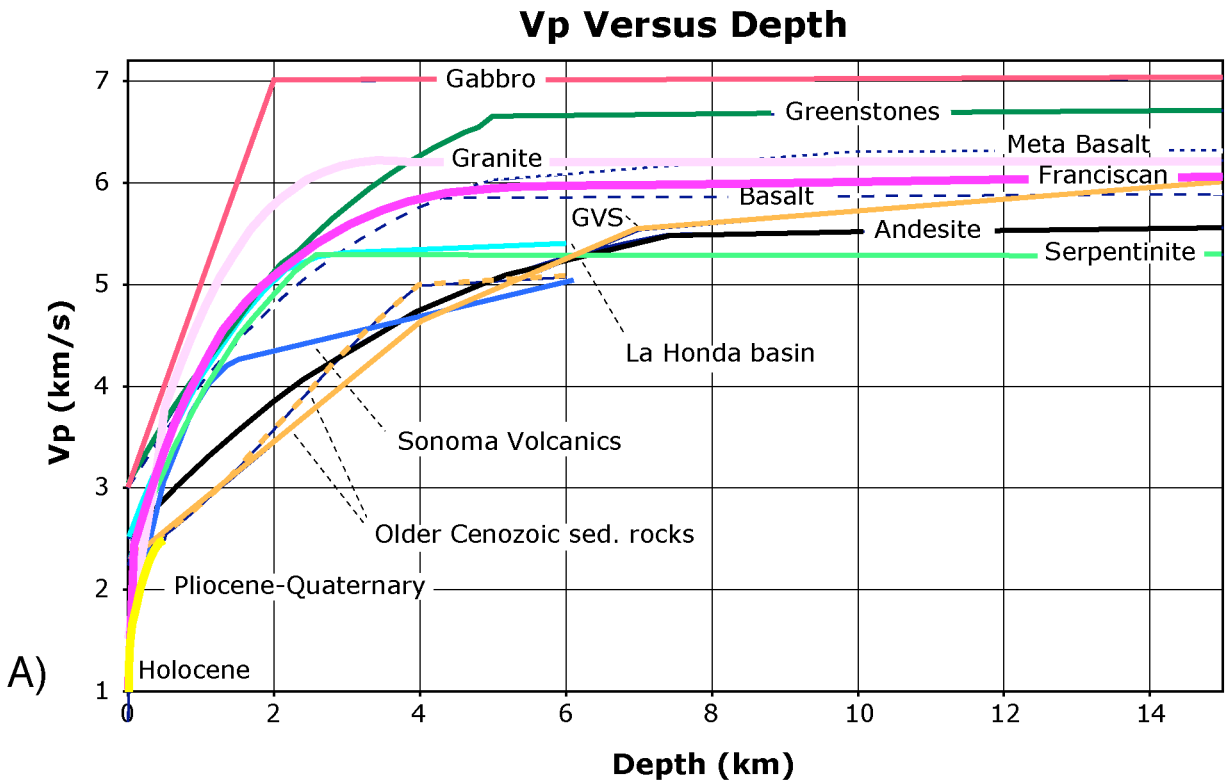

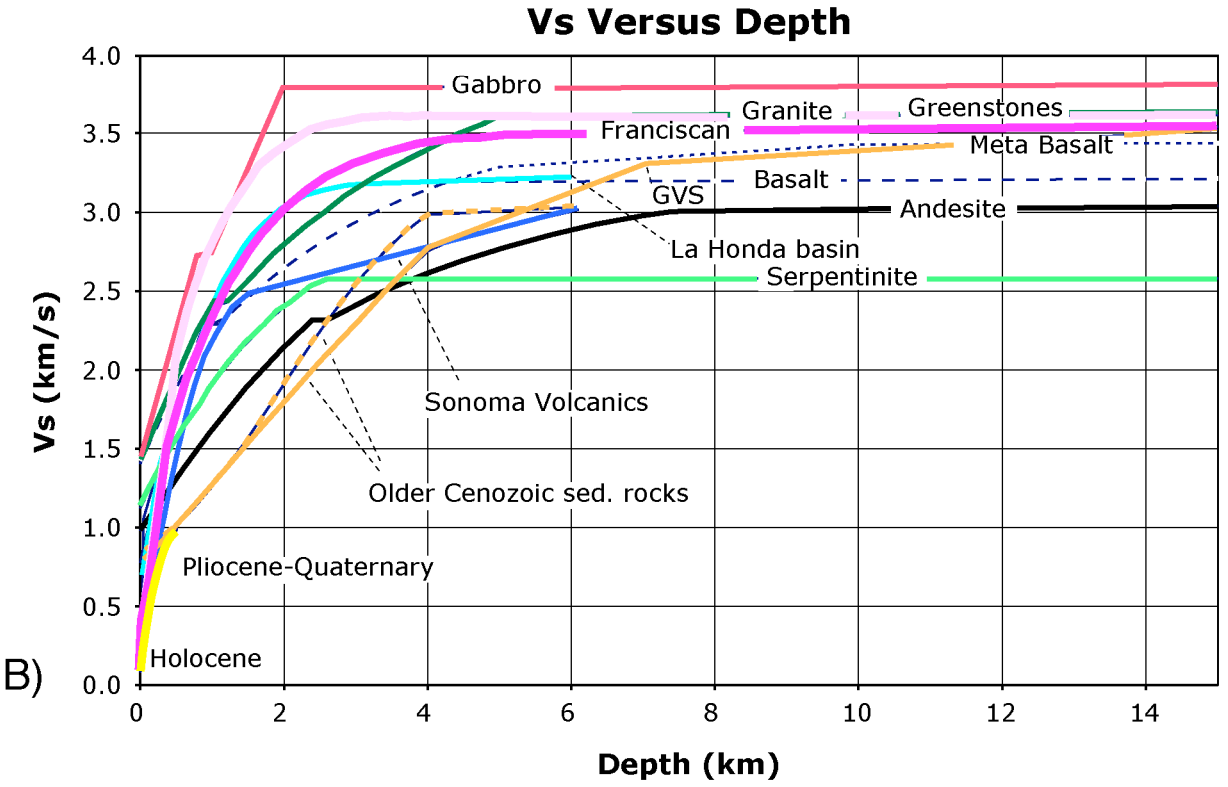

Figure 15. (A) Summary of the Vp versus depth relations for all the rock types reported here. (B) Summary of the Vs versus depth for all rock types reported here. Note that at higher velocities the relative order of the curves are different than in Figure 15A due to variations in the Vp/Vs ratio of the various rock types.